
Comparison of methods to determine extraction efficiencies of Ra isotopes and ^{227}Ac from large volume seawater samples

Léon Morgane ^{1,*}, Van Beek Pieter ¹, Sanial Virginie ², Souhaut Marc ¹, Henderson Paul ³, Charette Matthew A. ³

¹ Laboratoire d'Etudes en Géophysique et Océanographie Spatiale (LEGOS), Université de Toulouse, CNES/CNRS/IRD/Université Toulouse III Paul Sabatier, Toulouse, France

² Université de Toulon, Aix Marseille Univ., CNRS, IRD, MIO, Toulon, France

³ Department of Marine Chemistry and Geochemistry, Woods Hole Oceanographic Institution, Woods Hole, MA 02543, USA

* Corresponding author : Morgane Léon, email address : morgane.leon@univ-tlse3.fr

Abstract :

Radium isotopes, other than ^{226}Ra , and ^{227}Ac are typically present at low activities in the open ocean. The analysis of these isotopes thus requires collection of large volumes of seawater and high sensitivity, low background instruments. To obtain the required large volumes (hundreds to thousands of liters), these radionuclides are typically preconcentrated on cartridge-style filters impregnated with MnO_2 (Mn-cartridges) deployed on in-situ pumps. This technique, however, requires the determination of the extraction efficiency of the Mn-cartridges for the radionuclides of interest. For Ra isotopes, we used two methods to estimate the extraction efficiency of these Mn-cartridges at two stations on the South-West Indian Ridge in the Southern Ocean (GEOTRACES GS02). Method (1) compares the ^{226}Ra activities recovered on the Mn-cartridges versus the activities determined in Mn-fibers, through which seawater was passed at a flow rate $< 1 \text{ L min}^{-1}$ to quantitatively sorb Ra (Mn-fiber method) while method (2) combines the ^{226}Ra activities determined from two Mn-cartridges placed in series on in-situ pumps (A-B method). The second method is also applied to determine the ^{227}Ac extraction efficiency. We find a relatively wide-range of Ra and ^{227}Ac extraction efficiencies across the dataset (from 44.8% to 99.6% for Ra, and from 23.7% to 77.5% for ^{227}Ac). Overall, the yield of ^{227}Ac extraction is lower than that of Ra (mean value of $49.3 \pm 19.0\%$ for ^{227}Ac , $n = 10$; mean value of $79.2 \pm 10.3\%$ for Ra, $n = 13$, using the Mn-fiber method and a mean value of $63.9 \pm 12.5\%$, $n = 11$ using the A-B method). Our dataset suggests that the Ra extraction efficiencies using either the A-B method or the Mn-fiber method are in relatively good agreement. Consequently, the ^{223}Ra , ^{224}Ra and ^{228}Ra activities determined from the Mn-cartridges by applying the two Ra extraction yields are similar. We also show that the ^{227}Ac extraction efficiency can be estimated from the Ra extraction efficiency allowing the use of a single Mn-cartridge. Finally, we recommend to determine the Ra and ^{227}Ac extraction efficiencies in each individual Mn-cartridge, rather than applying a single extraction efficiency to all the Mn-cartridges, since a significant variability in the extraction efficiencies was observed between the different Mn-cartridges.

Highlights

► We compare methods to estimate Ra and ^{227}Ac extraction efficiency of Mn-cartridges. ► The Ra extraction efficiencies of the Mn-cartridges range from 44.8% to 99.6%. ► The ^{227}Ac extraction efficiencies are lower than those for Ra (23.7–77.5%). ► The ^{227}Ac extraction efficiency can be estimated from the Ra extraction efficiency.

Keywords : Radium, Actinium-227, Extraction efficiency, Methodology, Ocean, Tracers

1. Introduction

Radium (Ra) has four naturally occurring isotopes (^{224}Ra , $t_{1/2}$: 3.66 d; ^{223}Ra , $t_{1/2}$: 11.4 d; ^{228}Ra , $t_{1/2}$: 5.75 y; ^{226}Ra , $t_{1/2}$: 1600 y) continuously produced by radioactive decay of thorium (Th) isotope parents (^{228}Th , ^{227}Th , ^{232}Th , ^{230}Th , respectively) in the uranium-thorium decay series. While Th isotopes are strongly reactive to particles and preferentially adsorb onto mineral surfaces in marine systems (Cochran, 1982), Ra is easily released from surfaces or particles due to the high ionic strength and is therefore mostly found in the dissolved phase (Elsinger and Moore, 1980; Ku and Lin, 1976; Li and Chan, 1979; Moore, 1987). As Th and U are mainly present in soils, sediments and rocks, Ra isotopes in marine environment find their main source from diffusion from deep-sea sediments and continental shelves (Ku and Lin, 1976; Moore, 1969). Their concentrations in the ocean are thus widely dependent on the U and Th content in these sources.

The different half-lives of the Ra isotopes allow us to study chemical and physical processes in the ocean on different temporal and spatial scales (Annett et al., 2013; Charette et al., 2007; Dulaiova et al., 2009; Sanial et al., 2014; van Beek et al., 2008). Because of its relatively long half-life, ^{226}Ra is the most abundant Ra isotope with a total inventory in the oceans of about $4.78 \pm 0.27 \times 10^{18}$ Bq (IAEA, 1988; Hanfland, 2002; Neff, 2002) and is a historical tracer of water masses used to study the global scale deep ocean circulation (Broecker et al., 1976, 1967; Charette et al., 2016, 2016; Chung, 1987; Chung and Craig, 1980; Inoue et al., 2022; Ku et al., 1980; Ku and Lin, 1976; Le Roy et al., 2018). With a shorter half-life, ^{228}Ra is preferentially used as a tracer to study mesoscale and coastal processes at a time scale of years such as horizontal mixing between the continental shelves and the open ocean (Kaufman et al., 1973; Kipp et al., 2018a; Knauss et al., 1973; Sanial et al., 2018; Yamada and Nozaki, 1986), river inputs (Moore and Krest, 2004; Vieira et al., 2020), vertical mixing (Charette et al., 2007; van Beek et al., 2008), Submarine Groundwater Discharge (SGD; Kim et al., 2005; Li et al., 1980; Moore et al., 2008; Rodellas et al., 2017) or hydrothermal vents (Kadko, 1996; Kadko et al., 2007; Kadko and Butterfield, 1998; Kadko and Moore, 1988; Kipp et al., 2018b; Léon et al., *subm*). On the other hand, ^{227}Th (direct daughter of ^{227}Ac) and ^{228}Th (daughter of ^{228}Ra) are particle reactive (Cochran, 1982) and release ^{223}Ra and ^{224}Ra , respectively, in the dissolved phase by radioactive decay. With half-lives in the order of days, ^{223}Ra and ^{224}Ra are used to study coastal processes on the time scale of days or weeks, including the quantification of SGD fluxes (Bejannin et al., 2017; Garcia-Orellana et al., 2021; Tamborski et al., 2017), flushing rates in estuaries and above continental shelves (Léon et al., 2022; Moore and Krest, 2004) and horizontal or vertical mixing coefficients (Charette et al., 2007; Koch-Larrouy et al., 2015; Léon et al., *subm*). Aside from ^{226}Ra , which has a long half-life relative to ocean overturning timescales, Ra isotope activities generally decrease with increasing distance from their source due to mixing with seawater and radioactive decay. As such, intermediate waters tend to have lower activities of Ra isotopes than surface or bottom waters. Because the vertical mixing rate of the ocean is much slower than the mean life of ^{223}Ra , ^{224}Ra or even ^{228}Ra , little of the Ra isotopes can penetrate into the intermediate ocean (Moore, 1969) with the exception of regions impacted by hydrothermal vents (Kadko, 1996; Kadko et al., 2007; Kadko and Butterfield, 1998; Kadko and Moore, 1988; Kipp et al., 2018b; Léon et al., *subm*). Their concentrations are thus often below the detection limit in the mid water column away from the ocean boundaries (Charette et al., 2007; Sanial et al., 2015; van Beek et al., 2008). In seawater, activities of Ra isotopes usually range from ca. 0.1 to several tens of disintegrations per minute (dpm) per 100 kg of seawater.

The ^{227}Ac isotope ($t_{1/2}$: 21.8 years) is part of the ^{235}U radioactive series ($t_{1/2}$: $7.04 \cdot 10^8$ years). Due to its very long residence time in the oceans (~ 0.5 Ma; Ku et al., 1977), ^{235}U is uniformly distributed in the oceans (Weyer et al., 2008) leading to a constant production of ^{231}Pa ($t_{1/2}$: 32,760 years) by radioactive decay of ^{235}U in the water column. ^{231}Pa is preferentially scavenged onto particles and accumulates in sediments (Anderson et al., 1983). It decays into ^{227}Ac which is more soluble than its parents (Nozaki, 1993); it is thus partially released into the dissolved phase and then redistributed in the deepest part of the water column by mixing and transport. ^{227}Ac is thus mainly produced in deep waters and Nozaki (1984) was the first to propose ^{227}Ac as a deep-sea tracer. Since then, it has been used to trace deep ocean circulation on a basin scale (~ 100 years timescale) to quantify vertical eddy diffusivity coefficients (Geibert et al., 2002; Koch-Larrouy et al., 2015; Le Roy et al., 2023; Nozaki, 1984), to estimate upwelling rates (Geibert et al., 2002) or to trace hydrothermal system (Kipp et al., 2015; Moore et al., 2008b). Despite its recognized interest, research about ^{227}Ac remains difficult due to the low concentrations in the ocean. Geibert et al. (2008) thus estimated the total oceanic inventory of ^{227}Ac to be 37 mol, which is equivalent to about 8.4 kg ($2.25 \cdot 10^{16}$ Bq). Relatively few studies using ^{227}Ac are thus reported (Dulaiova et al., 2013; Geibert et al., 2008, 2002; Geibert and Vöge, 2008; Kipp et al., 2015; Koch-Larrouy et al., 2015; Le Roy et al., 2023, 2019; Levier et al., 2021; Nozaki, 1993, 1984; Shaw and Moore, 2002).

The analysis of Ra and ^{227}Ac isotopes in the ocean therefore requires the collection of large volumes of water (several hundred liters) followed by an extraction method. The need to preconcentrate large volumes of seawater has historically greatly limited the number of samples for Ra and Ac isotopes in the open ocean. The extraction of these radionuclides could be done either through coprecipitation of radium with barium sulfates (Gordon and Rowley, 1957), or through Fe or Mn hydroxide coprecipitation (Geibert and Vöge, 2008) or through sorption onto a media impregnated with MnO_2 (Shaw and Moore, 2002). Filtration through a media impregnated with MnO_2 is less constraining to setup and limit chemistry steps. Commonly, seawater is filtered through i) acrylic fibers impregnated with MnO_2 (Mn-fibers) at a flow rate below 1 L min^{-1} to ensure that 100 % of Ra and Ac are sorbed onto Mn-fibers (Moore and Reid, 1973) or through ii) acrylic cartridges impregnated with MnO_2 (Mn-cartridges) mounted on In-Situ Pumps (ISP) immersed for several hours to allow the filtration of hundreds of liters of seawater (Charette and Moran, 1999; Livingston and Cochran, 1987; Mann and Casso, 1984). On the one hand, the filtration of seawater through the Mn-fibers leads to a maximal extraction efficiency of the radionuclides but requires large volumes of water to be brought on board, usually using Niskin bottles mounted on a CTD rosette or a surface pump for upper water column sampling. This technique usually prevents from building vertical profiles with a high resolution and has thus often been applied for the analysis of ^{226}Ra (and sometimes ^{228}Ra) that can be conducted on relatively small volumes of seawater (~ 10 -20 L). On the other hand, the use of ISP allows the filtration of large volumes of water (> 300 L) but the flow rate is higher than the maximum value of 1 L min^{-1} that was shown to quantitatively sorb Ra from seawater. This latter method thus requires the quantification of the Ra extraction efficiency. To do so, one possibility is to mount a Niskin bottle above the ISP to compare the ^{226}Ra activity determined from the Niskin bottle (via Mn-fiber media) versus the activity determined from the ISP (via Mn-cartridge media) in a same cast (Charette et al., 2015). As the isotopes of a same element have identical chemical properties, the ^{226}Ra extraction efficiency can be applied to all Ra isotopes in a given sample. Livingston and Cochran (1987) developed another method to quantify radionuclides in open ocean waters by positioning two cartridges in series in ISP. The extraction efficiency of the radionuclides such as

Ra and Ac is thus achieved by comparing the activities determined on the two cartridges. The radionuclide activity in seawater is subsequently quantified by applying the efficiency to the activity observed in the first cartridge. However, extraction efficiency can vary with the cartridge properties, the water flow rate passing through the cartridge, and also potentially with environmental conditions.

In this study, we investigated the Ra and ^{227}Ac activities at two stations located in the Southern Ocean and visited during the GEOTRACES GS02 cruise (SWINGS cruise). At these two stations, we deployed Niskin bottles to collect ~12 L samples and ISP equipped with two Mn-cartridges placed in series to filter *in-situ* large volumes of seawater. This sampling scheme allows us to determine the yield of Ra extraction either by 1) comparing the ^{226}Ra activities determined in Mn-fibers with the ones determined in the first Mn-cartridge and (2) comparing the ^{226}Ra activities in the two Mn-cartridges in ISP. We therefore aimed to provide information 1) on the validity of the method based on the use of two cartridges placed in series that may sometimes be questioned due to the assumptions associated with this method and 2) on the best way to determine the Ra extraction efficiency. Subsequently, we used the second method (Mn-cartridges placed in series) to determine the extraction efficiency of ^{227}Ac , that we compared to the Ra extraction efficiency. Such comparison exercise has rarely been done because usually one single method is used for a dedicated cruise due to large seawater volumes needed and subsequent long analytical measurements to quantify the low concentrations of Ra isotopes and ^{227}Ac in the open ocean.

2. Material and methods

2.1. Study area

The samples were collected at two stations located above the South West Indian Ridge (SWIR) in the Southern Ocean during the GEOTRACES GS02 cruise, which took place on the R/V *Marion Dufresne* between South Africa and Heard Island (January -March 2021). Along the section, these two stations (Station 14, 1388 m, 44°51.690 S, 36°10.460 E; Station 15, 1770 m, 44°51.178 S, 36°13.841 E; Fig. 1) were suspected to be under the influence of hydrothermal vents (Léon et al., *subm.*; Baudet et al., *subm.*).

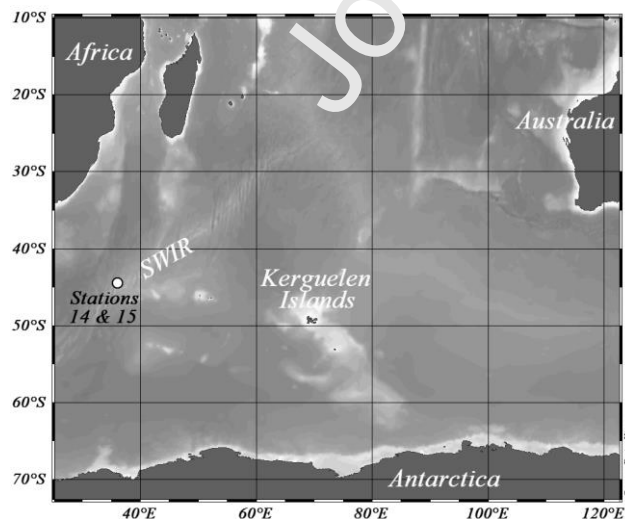


Figure 1: Map indicating the location of the stations 14 and 15 (open circle) investigated over the South West Indian Ridge in the Indian sector of the Southern Ocean.

2.2. Sampling method

First, water samples were collected using Niskin bottles mounted on a rosette and deployed at the same depths as the ISPs. These samples were designed to collect dissolved ^{226}Ra , which displays higher activities in seawater than ^{223}Ra , ^{224}Ra and ^{228}Ra , and can be analyzed in relatively small volumes (~12 L). Seawater from Niskin bottles were then passed by gravity through 10 g of MnO_2 impregnated acrylic fibers (Mn-fibers) placed into two small cartridges in series. The Mn-fibers were bought already impregnated to Scientific Computer Instruments and were “fluffed” to occupy the entire volume of the cartridges (Charette et al., 2012). The flow rate was set to 200 mL min^{-1} to quantitatively adsorb Ra isotopes (Moore and Reid, 1973). Between 11.2 and 21.8 L of seawater were collected per sample (Tab. 1). The Mn-fibers were then placed into plastic bags and rinsed three times with Ra-free water, to remove salt from seawater.

Second, Mn-cartridges were impregnated in the laboratory with MnO_2 using the following protocol derived from (Henderson et al., 2013). CUNO acrylic cartridges were cut to obtain cartridges of about $77 \pm 4 \text{ mm}$. After being dusted with compressed air, they were immersed in Ra free water for a minimum of 48 hours at room conditions (temperature of $20 \pm 2^\circ\text{C}$ and relative hygrometry of $60 \pm 10 \%$) in order to promote the future adsorption of manganese on the cartridges. The cartridges were then placed individually under vacuum in anti-permeation bags (SOREVAC ©; $80\mu\text{m}$ thick gasproof) containing 200 mL of saturated KMnO_4 solution (0.5 M) for 24 to 48 hours at room conditions to make the solution penetrate to the core of the cartridge. The cartridges were then immersed in 3 successive tanks of Ra free water before being individually rinsed to ensure that all the excess KMnO_4 was washed out. The so-called Mn-cartridges were then stored individually in plastic bags under vacuum and in the dark until use. These Mn-cartridges were then mounted on McLane ISP to preconcentrate *in-situ* dissolved Ra isotopes and ^{227}Ac from large volumes of seawater at different depths in the water column. A spring was placed under the Mn-cartridges into the ISP cartridge holder, in order to minimize seawater bypassing through the Mn-cartridge, especially at great depth where high pressure may reduce the size of the Mn-cartridges. Prior to passing through the Mn-cartridges, seawater was filtered through Supor ($0.8 \mu\text{m}$ pore size) or QMA (Whatman© $1 \mu\text{m}$ pore size) filters mounted on the ISPs. Eight ISPs were deployed at station 14 and six ISPs were deployed at station 15. The pumping duration was set for 3 hours and thus filtering through the Mn-cartridges between 427 and 677 L of seawater (with a mean flow rate ranging from 2.3 up to 3.7 L min^{-1} ; Tab. 1). The sampling resolution was increased near the seafloor because these samples were designed to trace the presence of a hydrothermal activity in the area. The yield of Ra fixation is unknown because the flow rate of seawater that passed through the Mn-cartridges is greater than the 1 L min^{-1} recommended to get a yield of 100%. Except for the three shallowest pumps at station 14 (50 m, 200 m, 900 m), two Mn-cartridges were mounted in series at each depth (A Mn-cartridge followed by a B Mn-cartridge), to provide information on the yield of Ra and ^{227}Ac fixation using the A-B method described in section 2.4 (Baskaran et al., 1993; Bourquin et al., 2008; Le Roy et al., 2019; Livingston and Cochran, 1987; Mann and Casso, 1984; van der Loeff and Moore, 1999). Each Mn-cartridges were rinsed with Ra-free water for ca. 10 minutes to remove salt from seawater. To do so, the Mn-cartridge holders were connected to two small cartridges placed in series, filled with Mn-fibers and themselves connected to the tap of the boat.

2.3. Analytical methods

2.3.1. Analysis of ^{223}Ra , ^{224}Ra and ^{227}Ac using RaDeCCs

The Mn-cartridges and Mn-fibers were analyzed using four Radium Delayed Coincidence Counter (RaDeCC, Scientific Computer Instruments, USA) systems. RaDeCCs display a very low background and are thus optimal equipment to quantify low seawater Ra and ^{227}Ac activities. Background measurements were regularly conducted on board and later in the laboratory. Background corrections were made considering the value determined at the same period as the sample counting. The RaDeCCs were calibrated using Mn-cartridges and Mn-fibers impregnated with ^{232}Th standards. Efficiencies for ^{219}Rn channel (used to quantify ^{223}Ra and ^{227}Ac activities) were estimated following calculations presented by Moore and Cai, (2013).

Each sample was analyzed for 6 to 24 hours with the RaDeCC system being flushed every 3 hours with air for 5 to 10 minutes before reintroducing helium. As ^{224}Ra and ^{223}Ra have short half-lives, they were measured on board within a few hours of sample collection to obtain the total ^{224}Ra ($^{224}\text{Ra}_{\text{tot}}$) and ^{223}Ra ($^{223}\text{Ra}_{\text{tot}}$) activities. A second measurement was conducted 21 days after sampling to determine the ^{224}Ra supported by ^{228}Th in the samples. Excess ^{224}Ra ($^{224}\text{Ra}_{\text{ex}}$) was determined by subtracting the supported activities from the $^{224}\text{Ra}_{\text{tot}}$ activities. A third counting was performed approximately 90 days after sample collection to quantify the ^{223}Ra supported by ^{227}Ac . The supported activities were subtracted from the $^{223}\text{Ra}_{\text{tot}}$ activities to determine excess ^{223}Ra activities ($^{223}\text{Ra}_{\text{ex}}$). Therefore the activities reported for short-lived Ra isotopes are $^{223}\text{Ra}_{\text{ex}}$ and $^{224}\text{Ra}_{\text{ex}}$. Error propagation calculations were conducted based on Garcia-Solsona et al. (2008).

To quantify ^{227}Ac activities on A Mn-cartridges, a total of 65 measurements ranging from 6 to 25 hours, flushed every 3 hours, were performed to study the associated errors (1 triplicate, 3 quadruplicates and 10 quintuplets; Fig. 2). Thus, the external precision is associated with the standard deviation (1SD) of the replicate measurements of a given sample, while the internal precision is defined as the uncertainty calculated by error propagation according to Garcia-Solsona et al. (2008). Internal precisions are < 0.059 dpm (1 SD) and the relative standard deviation (RSD) range from 20.1 % to 44.3 % with an average of 30.9 %. As a comparison, the external precision of these replicates is < 0.032 dpm (1SD) and the RSD range from 2.1 % to 58.6 %, with a weighted average of 17.4 % (weights of 3 for triplicates, 4 for quadruplicates, and 5 for quintuplets). With the exception of one sample (15_700m in Fig. 2), all measurements have an internal precision larger than the weighted average of external precision. This suggests that the uncertainties calculated by propagation (Garcia-Solsona et al., 2008) are likely overestimated. Therefore, we prefer to report the external precision rather than the internal precision.

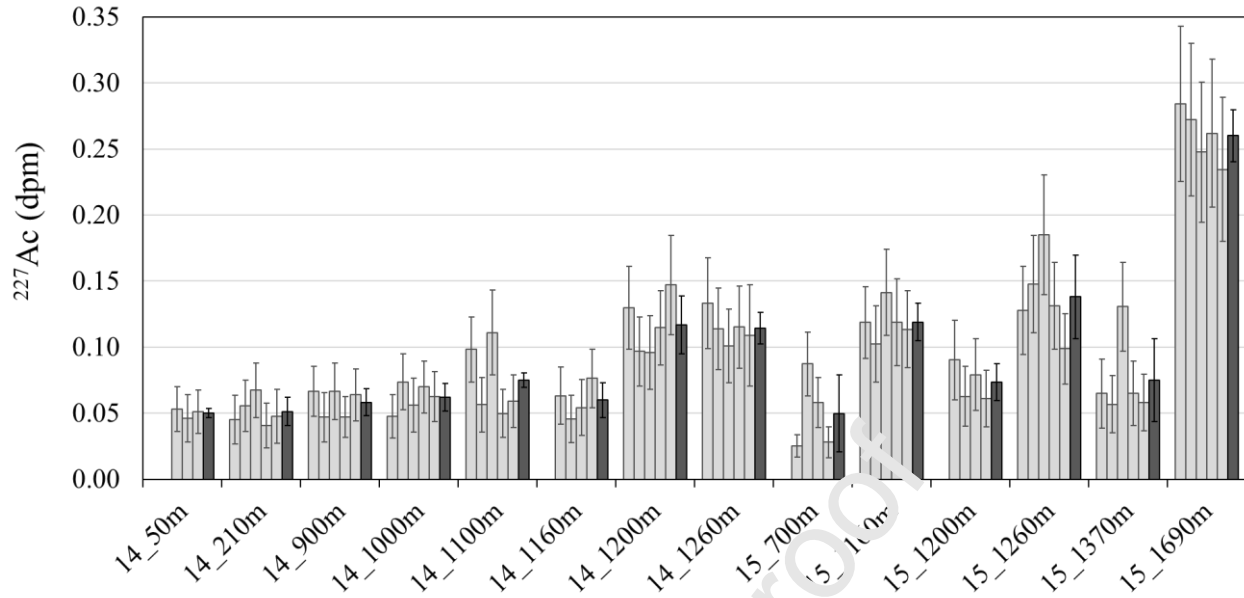


Figure 2: Repeatability of ^{227}Ac activities, in dpm, for the Mn-cartridges (light grey bars). Dark grey bars show the mean values of these activities with the standard deviation of the mean (1SD). The sample IDs are listed on the x-axis as follows “Station Number_depth”.

2.3.2. Analysis of ^{226}Ra and ^{228}Ra using gamma spectrometers

Following RaDeCC counting, Mn-cartridges were ashed at 450°C for 15 to 20 minutes to reduce their volume, and let to cool down under a ventilated hood. The ashes were then placed in plastic tubes that were sealed with epoxy resin to prevent any loss of ^{222}Rn . Mn-fibers were directly pressed and placed into plastic tubes. These tubes were also sealed with epoxy resin to prevent any loss of ^{222}Rn . The samples were left at least 3 weeks before analysis to reach secular equilibrium between ^{226}Ra and its daughters. The samples were analyzed using a SAGE-Well (MIRION-CANBERRA) germanium gamma spectrometer at the LAFARA laboratory in the French Pyrénées (van Beek et al., 2013) to determine the ^{226}Ra and ^{228}Ra activities. The detector has a volume of 450 cm^3 and a well diameter of 32 mm. It is located underground below 85 m of rock to protect it from cosmic radiation, thus providing a very low background. Due to the low activity levels in the samples, both Mn-cartridges and Mn-fibers were analyzed for at least 4 days. The detector was calibrated using standards provided by IAEA (RGU1 and RGTH1). ^{226}Ra was determined using ^{214}Pb peaks (294 keV and 352 keV) and ^{214}Bi peak (609 keV) and ^{228}Ra using ^{228}Ac peaks (339 keV and 969 keV). The uncertainties reported for the ^{226}Ra activities include counting statistics and uncertainty on the detection efficiencies (1SD).

2.3.3. Analysis of ^{226}Ra using ^{222}Rn -emanation technique

The Mn-fibers (~12 L samples) were analyzed for ^{226}Ra using the ^{222}Rn emanation technique at WHOI, USA. The method involves an extraction line for ^{222}Rn (daughter of ^{226}Ra , half-life: 3.8 days) followed by a scintillation cell (Key et al., 1979b, 1979a). First, the Mn-fibers were placed in PVC cartridges (Peterson et al., 2009) and flushed with helium. The cartridges were then sealed and held for at least 5 days to allow for radioactive growth of ^{222}Rn . The ^{222}Rn was then flushed out and cryo-trapped in a copper tube cooled with liquid nitrogen. After 15

minutes of ^{222}Rn accumulation in the copper tube, the ^{222}Rn was freed by heating the copper tube and further transferred into a Lucas cell by a helium flow. The Lucas cell was then placed into an alpha detector where it is counted from 3 to 6 hours. The counting system used for the cells is model AC/DC-DRC-MK 10-2. Uncertainties reported for ^{226}Ra include counting statistics and uncertainty on the detection efficiencies (1SD).

2.4. Extraction efficiencies of the Mn-cartridges

2.4.1. Mn-fiber method

The first method to quantify the Ra extraction efficiency of the Mn-cartridges is to compare the ^{226}Ra activities determined in the Mn-fibers (~12 L from Niskin bottles) using the ^{222}Rn emanation technique to the ^{226}Ra activity determined in the A Mn-cartridges (ISP) by gamma spectrometry. The Ra extraction efficiency of Mn-cartridges E_1 (Ra), can then be determined as follows:

$$E_1(\text{Ra}) = \frac{\text{Act}_A}{\text{Act}_{\text{Mn-fiber}}} \quad (1)$$

where Act_A and $\text{Act}_{\text{Mn-fiber}}$ are the ^{226}Ra activities (dpm 100L^{-1}) determined in the A Mn-cartridge and Mn-fiber, respectively (the volume considered here being the volume that passed onto the Mn-cartridge or the Mn-fiber, respectively). This efficiency can then be used to correct the activities determined in the Mn-cartridges for any of the other Ra isotopes that cannot be measured on small seawater volumes. The activity (dpm 100L^{-1}) of any Ra isotope in seawater (Act_{SW}) can thus be determined using the following equation:

$$\text{Act}_{\text{SW}} = \frac{\text{Act}_A}{E_1(\text{Ra})} \quad (2)$$

Note that in this study, the Niskin bottles and the ISPs were not deployed at the same time. We cannot exclude any temporal or spatial variability between the two samples, which may impact the estimate of the extraction efficiency. To prevent this potential bias, a Niskin bottle may be mounted directly above the ISP, so that the comparison between the two samples is more efficient (Charette et al., 2015).

2.4.2. A-B method

The second method to determine the Ra extraction efficiency (and potentially of other radionuclides such as Th and Ac) onto Mn-cartridges is based on the comparison of radionuclides activities from the two cartridges placed in series (A Mn-cartridge followed by B Mn-cartridge) mounted on the ISP (A-B method). This method was used in the past to quantify the activity of various radionuclides in the ocean (Fig. 3).

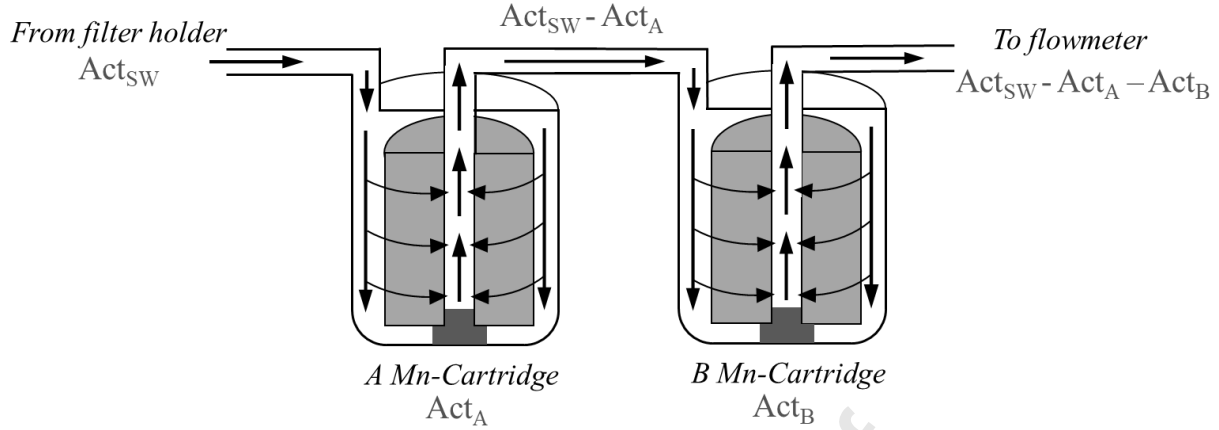


Figure 3: Cross-section of the two Mn-cartridges placed in series on in situ pumps. The shaded zones represent the Mn-cartridges placed within the Mn-cartridges holder. Arrows indicate the seawater flow passing through the Mn-cartridges. Act_A , Act_B and Act_{SW} are the radionuclide activities (dpm $100L^{-1}$) determined in the A Mn-cartridge, B Mn-cartridge and ambient seawater, respectively (the volume considered here being the volume that passed onto the Mn-cartridges).

In this case, seawater with a given activity (Act_{SW} , dpm $100L^{-1}$) first passes through the A Mn-cartridge. The activity on the A Mn-cartridge can thus be expressed as:

$$Act_A = Act_{SW} \times E_A \quad (3)$$

where Act_A is the activity (dpm $100L^{-1}$) retained onto the A Mn-cartridge and E_A the extraction efficiency of the A Mn-cartridge. The seawater leaving the A Mn-cartridge – with an activity equal to Act_{SW} minus Act_A – then passes through the B Mn-cartridge and exits the system with an activity equal to Act_{SW} minus that absorbed onto the two Mn-cartridges consecutively ($Act_{SW} - Act_A - Act_B$; Fig. 3). The activity of the B Mn-cartridge (Act_B , dpm $100L^{-1}$) is thus:

$$Act_B = (Act_{SW} - Act_A) \times E_B \quad (4)$$

where E_B is the extraction efficiency of the B Mn-cartridge. Assuming that the extraction efficiency for the A and B Mn-cartridges is the same ($E_A = E_B$), the extraction efficiency (E_2) for a given pair of Mn-cartridges can be determined as follows:

$$E_2 = 1 - \frac{Act_B}{Act_A} \quad (5)$$

In this study, E_2 (Ra) and E_2 (^{227}Ac) refer to Ra and ^{227}Ac extraction efficiencies, respectively, estimated by this A-B method. Note that in case the first Mn-cartridge becomes saturated with a radionuclide, the two cartridges may not behave similarly and the extraction efficiency may be distorted. However, the experience has shown the radionuclide sorption capacity of Mn-cartridges is maintained after passing up to several thousand of liters of seawater through them (Baskaran et al., 1993; Charette et al., 2007; Charette and Moran, 1999). The radionuclide activity (dpm $100L^{-1}$) in the water is then calculated with the following equation:

$$Act_{SW} = \frac{Act_A}{E_2} \quad (6)$$

Kemnitz (2018) has developed an alternative method which involves correcting the activity measured on the cartridges by taking into account the activity that is not retained by any of the two cartridges using the relationship:

$$Act_{SW} = \frac{Act_A + Act_B}{1 - f_{miss}} \quad (7)$$

where f_{miss} is the activity missed by both cartridges and equal to $(1 - E)^2$, where $(1 - E)$ is the fraction missed by one Mn-cartridge. This correction method will also be used in the following as a comparison.

3. Results

3.1. Ra extraction efficiency

3.1.1. Mn-fiber method

The ^{226}Ra activities determined in A Mn-cartridges and in Mn-fibers are shown in Fig. 4. The ^{226}Ra activities in Mn-fibers are invariably higher than those in the Mn-cartridges because the Mn-fibers quantitatively extract Ra (Moore and Reid, 1973). The Ra extraction efficiency - E_1 (Ra) - of the Mn-cartridges can be estimated for each sample by using Equation 1 (Tab 1). The extraction efficiencies thus range from 61.8 % to 89.6 % with an average of 79.2 ± 10.3 %, where the associated error of the mean extraction efficiency is the standard deviation (1SD, $n = 13$; Tab. 1; Fig. 4). The uncertainty of each extraction efficiencies was estimated by propagation of the uncertainties associated with the ^{226}Ra activities (1SD) of each Mn-cartridge and Mn-fiber (Tab.1). As a comparison, using the same method, Charette et al., (2015) estimated Ra extraction efficiencies of about 52 ± 22 % at an average flow rate of $\sim 6 \text{ L min}^{-1}$. Using Mn-cartridges manufactured by the same protocol as in Charette et al. (2015), Sanial et al. (2018) noted that the addition of a spring in the cartridge holder resulted in a better radium extraction efficiency of $66 \pm 16\%$ at a flow rate $\sim 6 \text{ L min}^{-1}$. The use of springs has likely contributed to the improvement of the extraction efficiency. As a consequence, the standard deviation of the mean extraction efficiency has also decreased which may point to an improved reproducibility of the process. Le Roy et al. (2019) reported an average of 60 ± 16 % (1SD, $n = 15$) at flow rate ranging from 3 to 6 L min^{-1} . We also note that the relatively low associated standard deviation may suggest a good reproducibility of the Mn impregnation on cartridges. McLane ISP with slightly lower flow rates were used in this study (mean flow rate of 3.3 L min^{-1}) when compared to other studies which may have improved the extraction efficiency onto the Mn-cartridges (Charette and Moran, 1999; Henderson et al., 2013). The variability of the extraction efficiencies observed in the different studies may thus be related to differences in the average flow rate and potentially also to different Mn-cartridge properties (composition -polypropylene or acrylic, size or degree of MnO_2 impregnation). Possible causes explaining the variability of the extraction efficiencies from one Mn-cartridge to the other will be discussed below (section 4.2.).

Table 1: ^{226}Ra activities (in $\text{dpm } 100\text{L}^{-1}$) determined in Mn-fibers and in A and B Mn-cartridges; the extraction efficiencies E_1 (Ra) (derived from Equation 1) and E_2 (Ra) (derived from Equation 5)

determined for each depth are also reported. No data were available (n.a.) at 500 m at station 15 (Mn-fibers) and at 50, 210, 900 m depth at station 14 (Mn-cartridges).

Station	Depth (m)	^{226}Ra		^{226}Ra		Extraction efficiency		
		Volume (L)	Mn-fibers ($\text{dpm } 100\text{L}^{-1}$)	Volume (L)	A Mn-cartridge ($\text{dpm } 100\text{L}^{-1}$)	B Mn-cartridge ($\text{dpm } 100\text{L}^{-1}$)	E_1 (%)	E_2 (%)
14	50	11.6	11.1 ± 0.3	427	10.5 ± 0.13	n.a.	94.5 ± 2.8	n.a.
	210	12.4	13.2 ± 0.2	601	11.2 ± 0.12	n.a.	84.8 ± 1.7	n.a.
	900	12.4	15.3 ± 0.6	615	11.2 ± 0.07	n.a.	73.5 ± 3.1	n.a.
	1000	11.6	17.3 ± 0.8	528	10.7 ± 0.12	5.5 ± 0.08	61.8 ± 3.1	48.1 ± 0.9
	1100	11.5	15.5 ± 0.4	548	13.4 ± 0.14	4.7 ± 0.08	86.8 ± 2.5	65.4 ± 1.2
	1160	11.6	14.2 ± 0.7	584	11.0 ± 0.12	6.1 ± 0.08	77.4 ± 3.7	44.8 ± 0.8
	1200	11.7	16.8 ± 0.2	674	11.8 ± 0.12	4.6 ± 0.07	70.5 ± 1.0	61.3 ± 1.1
	1260	11.6	15.5 ± 0.3	646	11.2 ± 0.11	5.1 ± 0.08	72.1 ± 1.7	54.5 ± 1.0
15	700			532	10.6 ± 0.12	3.9 ± 0.07	n.a.	62.9 ± 1.3
	1160	10.9	15.8 ± 0.4	579	15.8 ± 0.15	2.2 ± 0.06	99.6 ± 2.5	86.3 ± 2.2
	1200	11.3	16.6 ± 0.3	503	13.1 ± 0.14	4.4 ± 0.08	79.3 ± 1.8	66.7 ± 1.3
	1260	11.1	17.5 ± 0.9	665	14.2 ± 0.14	4.0 ± 0.06	81.2 ± 4.4	71.6 ± 1.3
	1370	11	16.2 ± 0.3	677	12.1 ± 0.12	4.5 ± 0.07	74.9 ± 1.7	61.7 ± 1.1
	1690	10.9	17.4 ± 0.3	630	12.8 ± 0.13	2.6 ± 0.05	73.4 ± 1.5	79.5 ± 1.6
							Mean	79.2 ± 10.3

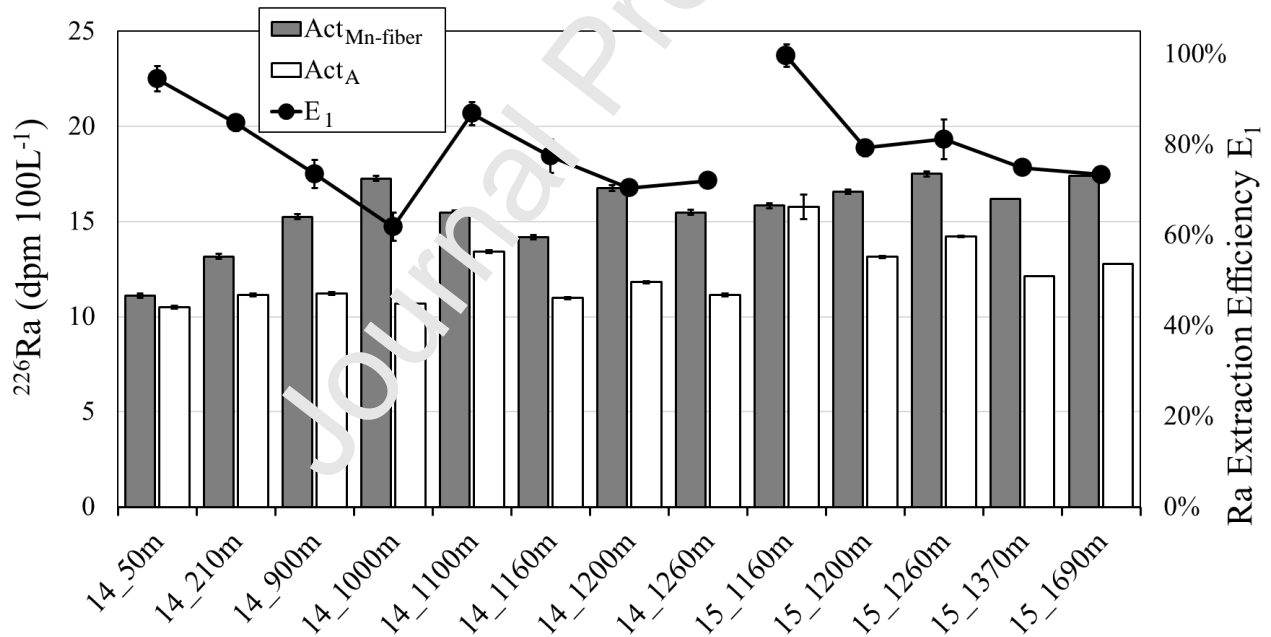


Figure 4: Estimate of the Ra extraction efficiency – E_1 (Ra) – using the Mn-fiber method. The ^{226}Ra activities in the Mn-fibers ($\text{Act}_{\text{Mn-fiber}}$, in $\text{dpm } 100\text{L}^{-1}$) are shown as dark grey bars and the ^{226}Ra activities in the A Mn-cartridges (Act_A , in $\text{dpm } 100\text{L}^{-1}$) are shown as white bars. The Ra extraction efficiencies E_1 (Equation 1) determined by comparing Mn-fibers and A Mn-cartridges activities are shown as black dots. The sample IDs are listed on the x-axis as follows “Station Number_depth”.

3.1.2. A-B method

The ^{226}Ra activities determined in B Mn-cartridges are always significantly lower than those determined in A Mn-cartridges, which is expected since seawater first passes through the A Mn-cartridge and then through the B Mn-cartridge (Tab. 1; Fig. 5). The E_2 (Ra) calculated using Equation 5 range from 44.8 % to 86.3 % with an average of 63.9 ± 12.4 %, where the associated error of the mean extraction efficiency is the standard deviation (1SD; $n = 11$; Tab. 1). Uncertainties of each extraction efficiencies was estimated by propagation of the uncertainties associated with the ^{226}Ra activities (1SD) of each Mn-cartridge (Tab.1). We note that the extraction efficiencies thus determined are slightly lower at station 14 (mean of 54.8 %) than at station 15 (mean of 71.5 %), even if average flow rates are similar at the two stations ($\sim 3.2 \text{ L min}^{-1}$). This pattern was not observed when using the Mn-fiber method (Fig.4) and is thus difficult to explain.

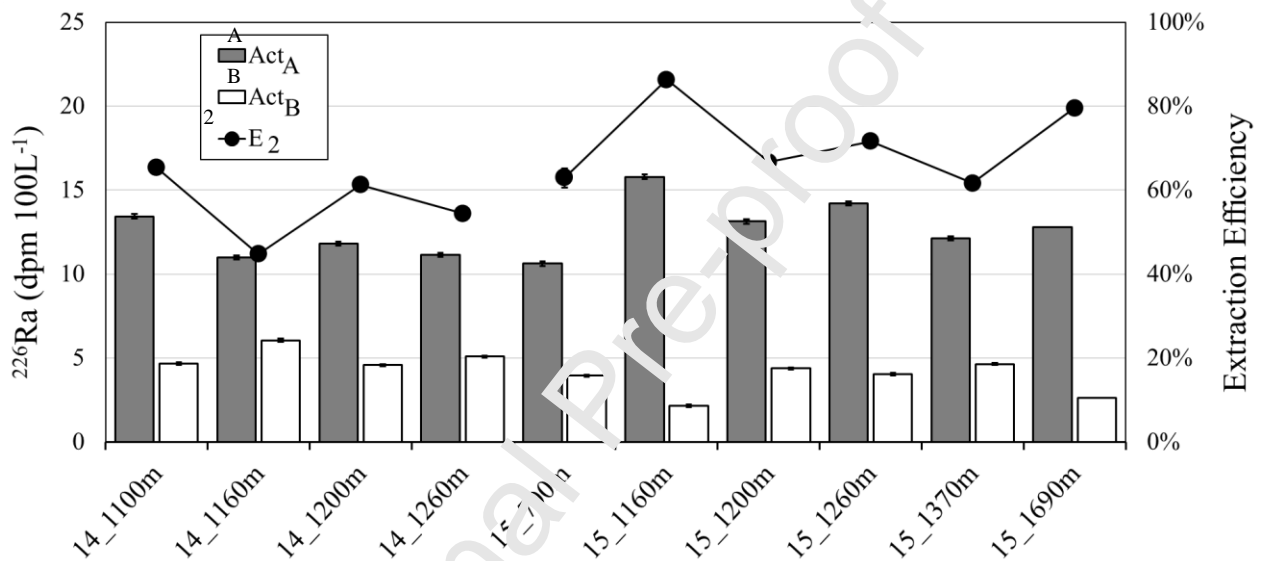


Figure 5: Estimate of the Ra extraction efficiency - E_2 (Ra) - using the A-B method, The ^{226}Ra activities in the A Mn-cartridges ($^{226}\text{Ra Act}_A$, in $\text{dpm } 100\text{L}^{-1}$) are shown as dark grey bars and the ^{226}Ra activities in the B Mn-cartridges ($^{226}\text{Ra Act}_B$, in $\text{dpm } 100\text{L}^{-1}$) are shown as white bars. The Ra extraction efficiencies E_2 (Equation 5) determined by comparing A and B Mn-cartridges are shown as black dots. The sample IDs are listed on the x-axis as follows "Station Number_depth".

3.2. ^{227}Ac extraction efficiency

We used the A-B method to quantify the ^{227}Ac extraction efficiency and named it as E_2 (^{227}Ac). As for Ra, we compare the ^{227}Ac activities determined in the A Mn-cartridges with those determined in the B Mn-cartridges. Activities determined in B Mn-cartridges are always lower than those determined in A Mn-cartridges (Fig. 6; Tab.2). However, in contrast to Ra, it was not possible to compare these results with the Mn-fiber method, since ^{227}Ac could not be determined in our small volume samples due to its lower concentration. Fig. 6 shows E_2 (^{227}Ac) ranging from 23.7 % to 77.5 %, with a mean value of 49.3 ± 19 %, where the associated error of the mean extraction efficiency is the standard deviation (1SD, $n = 10$). The uncertainty of each extraction efficiency was estimated by propagation of the uncertainties associated with the ^{226}Ra activities (1SD) of each Mn-cartridge. The extraction efficiencies display a larger variability compared to

the Ra extraction efficiencies. Note that several activities reported here, especially on the B Mn-cartridges, are very low, thus resulting in relatively high associated errors. As observed with the E_2 (Ra) (Fig. 5), we note that E_2 (^{227}Ac) are on average lower at station 14 (34.4 %) than at station 15 (64.3 %), even if the average flow rates are the same at the two stations.

Table. 2: ^{227}Ac activities determined in the A and B Mn-cartridges (Act_A and Act_B , respectively, in $\text{dpm } 100\text{L}^{-1}$) together with the extraction efficiency - E_2 (^{227}Ac) - deduced from Equation 5.

Station	Depth (m)	Volume (L)	^{227}Ac		Extraction Efficiency $E_2(^{227}\text{Ac})$ (%)
			A Mn-cartridge ($\text{dpm } 100\text{L}^{-1}$)	B Mn-cartridge ($\text{dpm } 100\text{L}^{-1}$)	
14	1000	528	0.013 ± 0.002	0.008 ± 0.002	34.8 ± 8.3
	1100	548	0.015 ± 0.003	0.012 ± 0.002	23.7 ± 6.4
	1160	584	0.009 ± 0.002	0.006 ± 0.001	38.9 ± 11.2
	1200	674	0.018 ± 0.003	0.009 ± 0.002	50.7 ± 13.3
	1260	646	0.021 ± 0.004	0.016 ± 0.002	25.8 ± 5.5
15	1160	579	0.022 ± 0.003	0.005 ± 0.001	75.4 ± 19.2
	1200	503	0.016 ± 0.003	0.007 ± 0.002	56.4 ± 17.0
	1260	665	0.022 ± 0.004	0.009 ± 0.002	58.5 ± 14.7
	1370	677	0.013 ± 0.003	0.006 ± 0.001	53.5 ± 16.2
	1690	630	0.043 ± 0.007	0.010 ± 0.002	77.5 ± 18.1
Mean					49.3 ± 19.0

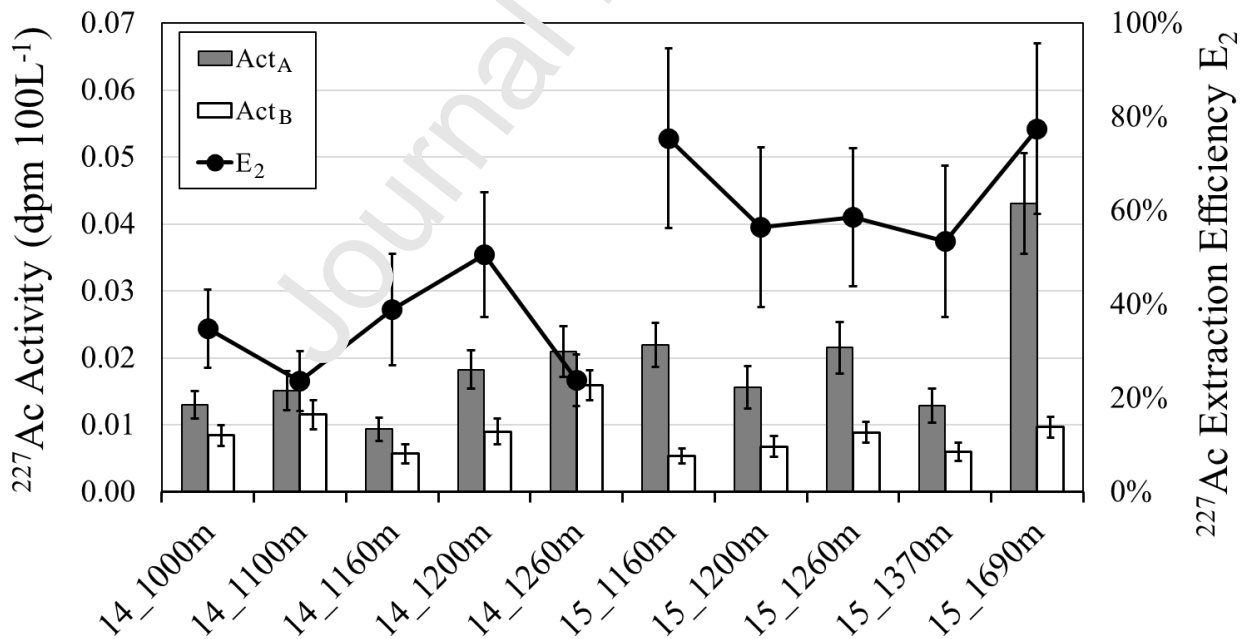


Figure 6: Estimate of the ^{227}Ac extraction efficiency - E_2 (^{227}Ac) - using the A-B method. The ^{227}Ac activities in the A Mn-cartridges (Act_A , in $\text{dpm } 100\text{L}^{-1}$) are shown as dark grey bars and the ^{227}Ac activities in the B Mn-cartridges (Act_B , in $\text{dpm } 100\text{L}^{-1}$) are shown as white bars. The ^{227}Ac extraction

efficiencies $E_2 - E_2(^{227}\text{Ac})$ - (Equation 5) determined by comparing A and B Mn-cartridges are shown in back dots. The sample IDs are listed on the x-axis as follows “Station Number_depth”.

Le Roy et al. (2019) also used acrylic Mn-cartridges produced with a similar protocol and reported $E_2(^{227}\text{Ac})$ that ranged from 31% to 78 %, with an average of 47 ± 12 % (1SD, $n = 21$). These extraction efficiencies are consistent with the values reported in this study (Tab. 2). Kemnitz (2022) reported values of about 54 % ($n \sim 30$) using acrylic Mn-cartridges (same as in this study). Using polypropylene Mn-cartridges, Geibert et al. (2002) and Geibert and Vöge (2008) reported extraction efficiencies of 69 ± 11 % ($n = 31$) and 77 ± 13 % ($n = 31$), respectively. Note that these authors used larger Mn-cartridges. Kipp et al. (2015) proposed to estimate the ^{227}Ac extraction efficiency by averaging the Ra and Th extraction efficiencies at each depth. These authors thus reported efficiencies ranging from 27.3 % to 74.4 %.

4. Discussion

4.1. Comparison of the Ra and ^{227}Ac extraction efficiencies

The Ra extraction efficiencies E_1 and E_2 , determined using the two different methods, are compared on Fig. 6 7 and 78. Overall, a relatively good agreement is observed between the two methods suggesting that the A-B method provides relatively good estimates of the Ra extraction efficiency. We note, however, that the extraction efficiencies calculated with the A-B method - $E_2(\text{Ra})$ - are slightly lower than those estimated by the Mn-fiber method- $E_1(\text{Ra})$.

Fig. 7 compares the Ra extraction efficiencies - $E_1(\text{Ra})$ and $E_2(\text{Ra})$ - with the ^{227}Ac extraction efficiencies $E_2(^{227}\text{Ac})$. With the exception of the sample collected at 1690 m depth at station 15, the Ra extraction efficiencies are invariably higher than the ^{227}Ac extraction efficiencies determined in the same Mn cartridges. Fig. S1 in supplementary material shows the relationship between $E_2(^{227}\text{Ac})$ and $E_2(\text{Ra})$.

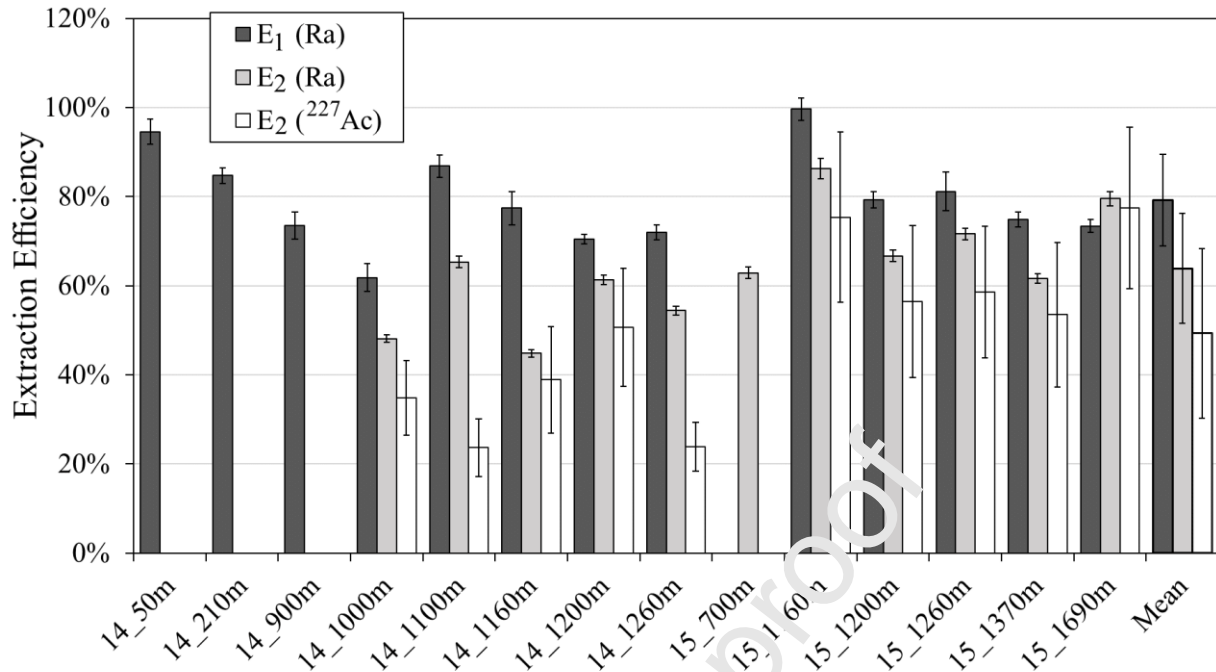


Figure 7: Comparison of Ra and ^{227}Ac extraction efficiencies. E_1 (Ra) are shown in dark grey bars, E_2 (Ra) in light grey bars and E_2 (^{227}Ac) in white bars. The mean extraction efficiency of each method is reported in the right of the figure. The sample IDs are listed on the x-axis as follows “Station Number_depth”. Only one cartridge was deployed at 50, 210, and 900 m for station 14, and at 700 m at station 15 preventing us from determining the extraction efficiency E_2 .

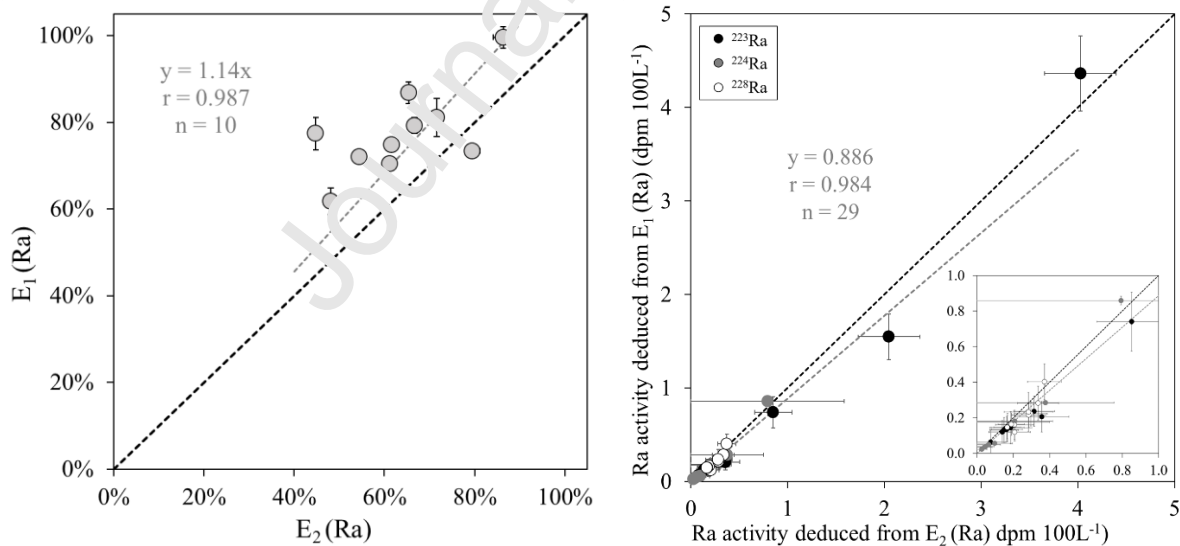


Figure 8: Left panel: Comparison of the Ra extraction efficiencies, E_2 (Ra) as a function of E_1 (Ra); right panel: Comparison of the Ra activities determined from E_1 (Ra) with the Ra activities determined from E_2 (Ra). The ^{223}Ra activities are in black dots, the ^{224}Ra activities are in grey dots and the ^{228}Ra activities are in white dots at stations 14 and 15. The black dashed line shows the 1:1 relationship while the grey dotted line shows the linear regression forced by the origin.

The relationship shown on Fig. 8 suggests that the E_2 (Ra) are on average 21 % lower than the E_1 (Ra) ($r = 0.987$, $n = 10$, p -value < 0.001). Fig. 8 compares the ^{223}Ra , ^{224}Ra and ^{228}Ra activities determined using the two extraction efficiencies (E_1 or E_2). We observe that although E_2 (Ra) is slightly lower than E_1 (Ra), it does not have a significant impact on the final Ra activities regardless of the Ra isotope ($r = 0.984$; $n = 29$, p -value < 0.001), probably due to the relatively large uncertainties of the Ra activities determined using these methods. The correlation holds true when individual Ra isotopes are considered ($r = 0.983$, $n = 10$, p -value < 0.001 for ^{223}Ra ; $r = 0.984$, $n = 9$, p -value < 0.001 , for ^{224}Ra ; $r = 0.986$, $n = 10$, p -value < 0.001 for ^{228}Ra).

On Fig. 9, we now compare the ^{227}Ac activities determined using either equation 6 that involves the extraction efficiencies determined from the A-B method or equation 7, following Kemnitz (2018). In the first method, the extraction efficiencies are determined in each individual Mn-cartridge (Tab.2), whereas Kemnitz (2018) use an average correction applied to all samples. Another difference is that the extraction efficiencies are applied to the sole A Mn-Cartridge to determine the ^{227}Ac activities for the first method, whereas, in the method of Kemnitz (2018), the ^{227}Ac activities are determined by summing the activities determined in the A and B Mn-cartridges. In this study, the average ^{227}Ac fraction missed f_{miss} is $15 \pm 3\%$ ($n=10$). This value is obtained by plotting the ^{227}Ac activities in the B Mn-cartridges versus A Mn-cartridges (Kemnitz, 2018). Note that the average ^{226}Ra fraction missed f_{miss} thus calculated is $11 \pm 1\%$ ($n=11$). Slightly higher activities using equation 6 are observed, but overall, we observe a relatively good agreement between the two estimates ($r = 0.965$, $n = 10$, p -value < 0.001). However, if we apply the method of Kemnitz (2018) to each individual samples (by calculating a f_{miss} factor to each sample, rather than applying an average correction to all samples) we find the same ^{227}Ac activities between the two methods.

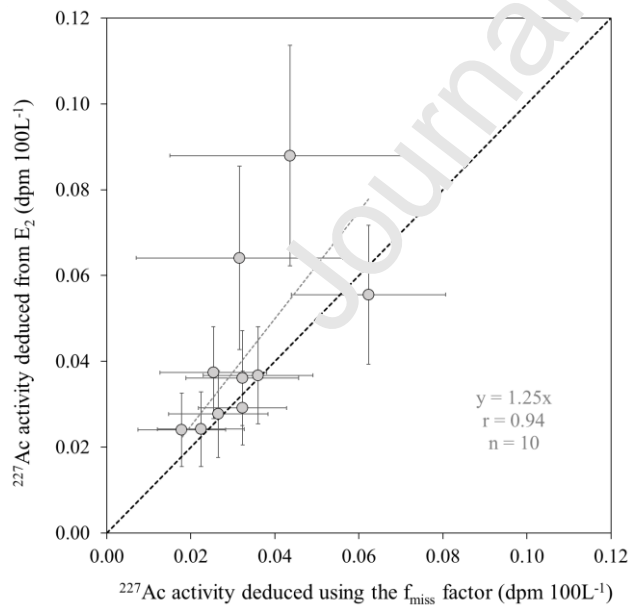


Figure 9: Comparison of the ^{227}Ac activities determined by correcting Act_A by E_2 (^{227}Ac) (equation 6) as a function of the ^{227}Ac activities estimated by correcting Act_A and Act_B by the missing factor f_{miss} following Kemnitz et al. (2018) (equation 7). The black dashed line shows the 1:1 relationship while the grey dotted line shows the linear regression forced by the origin.

4.2. Hypotheses that could explain the extraction efficiency variability

Overall, a relatively good agreement is observed between the two methods suggesting that the A-B method provides similar estimates of the Ra extraction efficiency ($r = 0.987$, $n = 10$, p -value < 0.001). We observe, however, a high variability in the extraction efficiency estimates from one sample to the other, independently from the method used. One can invoke the following hypotheses to explain the extraction efficiency variability between the Mn-cartridges.

The Mn impregnation on cartridges may vary from one sample to the other. We cannot exclude that CUNO acrylic cartridges may display slightly different shapes, even before being impregnated with KMnO_4 . Variability in the porosity of the cartridges could lead to a different KMnO_4 adsorption onto the cartridges, thus leading to variable Ra adsorption onto the Mn-cartridges.

The increase of pressure with increasing depth may impact the shape of the Mn-cartridge or impact its position in the cartridge holder which could in turn impact the water flow through the Mn-cartridge. No relationship, however, was observed between $E_1(\text{Ra})$, $E_2(\text{Ra})$ or $E_2(^{227}\text{Ac})$ and sample depth. As sample depth has a major influence on the pressure encountered by the Mn-cartridges, this suggests that pressure does not explain at first order the extraction efficiency variability. In this study, we placed springs in the cartridge holders below the Mn-cartridges to prevent seawater from flowing without passing through the Mn-cartridge. There may also be a temperature effect having a positive effect on adsorption kinetics at high temperatures. However, temperature does not seem to be an important factor in this study, since we observe no relationship between temperature and $E_1(\text{Ra})$, $E_2(\text{Ra})$ or $E_2(^{227}\text{Ac})$. Another factor that could influence the extraction efficiency is the seawater flow rate through the Mn-cartridges during *in-situ* pumping (Moore and Reid, 1973). The water flow through the Mn-cartridges may vary from one Mn-cartridge to the other and may vary through time during filtration. Preferential pathways may also exist within the cartridge holder. Factors that can reduce the flow rate include: filter clogging at the ISP inlet, the power decrease of the ISP batteries, or pressure that could possibly reduce the size of the Mn-cartridge, making water circulation through Mn-cartridges more difficult. A decrease in the water flow would increase the extraction efficiencies. However, no relationship was observed between $E_1(\text{Ra})$, $E_2(\text{Ra})$ or $E_2(^{227}\text{Ac})$ and the mean flow rate during filtration. As no correlation is observed between extraction efficiencies and depth, temperature or flow rate, this variability is likely best explained by the variability in the Mn impregnation on cartridges.

Finally, we note that the extraction efficiencies calculated with the A-B method - $E_2(\text{Ra})$ - are slightly lower than those estimated by the Mn-fiber method - $E_1(\text{Ra})$. The A-B method allows us to determine extraction efficiencies based on two Mn-cartridges placed in series, assuming that they have the same extraction efficiency. This latter assumption may not hold completely true. Another explanation that could explain this almost systematic difference between both methods ($E_1(\text{Ra})$ and $E_2(\text{Ra})$) is that some of the Ra present on the Mn-cartridges may partially desorb. When seawater passes through the Mn-cartridges and especially at high flow rates, some of the Ra present on the A Mn-cartridges may be removed (e.g., desorption of radium, leaching of Mn, ...) and may then adsorb onto the B Mn-cartridges, potentially compensating the leaching of the Ra out of the B Mn-cartridges. This process would reduce the difference in Ra adsorbed between

the two Mn-cartridges and would then reduce the extraction efficiencies determined using the A-B method (E_2).

4.3. Estimation of ^{227}Ac extraction efficiency from E_1 (Ra)

Based on our dataset, the Ra extraction efficiencies are slightly higher than the ^{227}Ac extraction efficiencies (Fig. 7). Here we evaluate if the ^{227}Ac extraction efficiency can be determined from the Ra extraction efficiency, using E_1 (Ra) as the reference. The E_2 (^{227}Ac) : E_1 (Ra) ratio is on average 0.64 ± 0.23 (1SD, $n=10$). This suggests that the ^{227}Ac extraction efficiency E_3 may be estimated as follows:

$$E_3(^{227}\text{Ac}) = 0.64 \times E_1(\text{Ra}) \quad (8)$$

The ^{227}Ac activity in seawater $Act_{\text{sw}}(^{227}\text{Ac})$ may thus be determined as follows:

$$Act_{\text{sw}}(^{227}\text{Ac}) = \frac{Act_A(^{227}\text{Ac})}{E_3} = \frac{Act_A(^{227}\text{Ac})}{0.64 \times E_1(\text{Ra})} \quad (9)$$

The uncertainties associated with E_3 (^{227}Ac) are estimated by error propagation of ^{227}Ac activities and E_1 (Ra). Fig. 10 shows the ^{227}Ac activities determined using the ^{227}Ac extraction efficiency deduced from E_3 (^{227}Ac) (equation 9) versus the ^{227}Ac activities determined from E_2 (^{227}Ac) at each depth (equation 6). We find that there is a relatively good agreement between the two activities ($r=0.929$, $n=13$, $p\text{-value} < 0.001$). If we exclude the three values that show a higher discrepancy (i.e., samples characterized by an ^{227}Ac efficiency determined with the A-B method too different from the mean value of 0.64), the correlation is improved ($r=0.989$, $n=10$, $p\text{-value} < 0.001$). In both cases ($n=10$ or $n=13$), no significant differences were observed ($p\text{-value} < 0.001$). However, note that in this latter case we cannot conclude which efficiency is most adapted (E_2 or E_3), since the ^{227}Ac extraction efficiency could not be compared with the Mn-fiber method as it was the case for Ra.

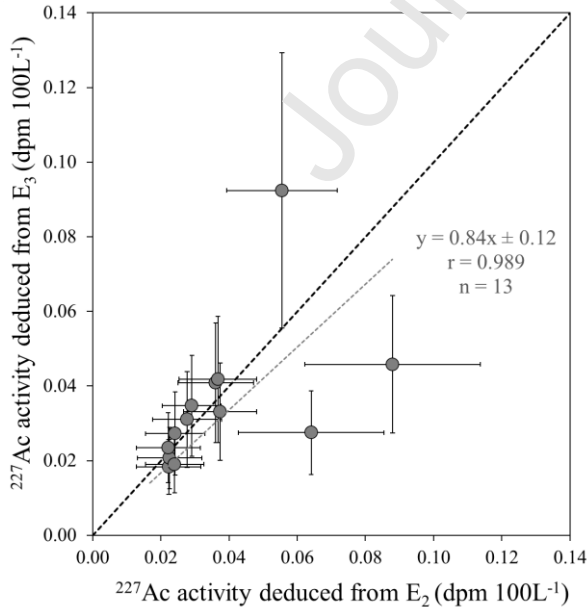


Figure 10: Comparison of the ^{227}Ac activities determined from the A-B method E_2 (^{227}Ac) with the ^{227}Ac activities determined from the E_1 (Ra) extraction efficiency, corrected as described in section 4.2. The black dashed line shows the 1:1 relationship while the grey dotted line shows the linear regression forced by the origin.

5. Conclusion

Because they are present at very low concentrations in the ocean, Ra isotopes and ^{227}Ac require the collection of large volumes of seawater, thus considerably limiting the construction of vertical profiles with a high resolution. Mn-cartridges mounted on in-situ pumps are thus commonly used to preconcentrate these isotopes from large seawater volumes (hundreds of liters). This technique, however, requires that the extraction efficiencies of the Mn-cartridges for these radionuclides are determined. Alternatively, Mn-fibers can be used to quantitatively preconcentrate Ra isotopes when seawater is passed at a flow rate $< 1 \text{ L min}^{-1}$. This latter technique is generally used to mainly determine ^{226}Ra activities since the determination of ^{223}Ra , ^{224}Ra , ^{228}Ra and ^{227}Ac activities in open ocean waters requires larger volumes of seawater. In this work, we evaluated the extraction efficiencies of the Mn-cartridges (1) by comparing the activities of the Mn-fibers versus the Mn-cartridges (Mn-fiber method) and (2) by comparing the activities determined in two cartridges placed in series on in-situ pumps (A-B method).

We estimated Ra extraction efficiencies ranging from 61.8 to 99.6 % (mean of 79.2 ± 10.3 %) using the Mn-fiber method and ranging from 44.8 to 86.3 % (mean of 63.9 ± 12.4 %) using the A-B method. Although the Ra extraction efficiencies are slightly lower when using the A-B method, the results obtained here tend to confirm the reliability of the A-B method to estimate extraction efficiencies. We also used the A-B method to quantify the ^{227}Ac extraction efficiency of the Mn-cartridges. Here, we report ^{227}Ac extraction efficiencies ranging from 23.7 to 77.5 (mean of 49.3 ± 19 %) which are significantly lower than the Ra extraction efficiency (by a factor of 0.64, when compared to the mean Ra extraction efficiency). These results suggest that the ^{227}Ac extraction efficiency may be estimated from the Ra extraction efficiency. However, more studies are required before it can be concluded that a constant factor exists between the Ra and ^{227}Ac extraction efficiencies from Mn-cartridges mounted on ISP. Finally, because the extraction efficiencies of the Mn-cartridges were shown to vary from one sample to the other, we recommend that the efficiencies are quantified in each individual sample rather than using a mean efficiency that would be applied to all samples. Among the factors that can influence the extraction efficiencies, one can mention seawater flow rate, temperature or pressure. None of these factors were shown to correlate with the extraction efficiencies, suggesting that the variability in the Mn impregnation on cartridges may explain the variability in the extraction efficiencies. We cannot exclude that preferential pathways exist in some cases within the cartridge holder. We recognize that in this study, only a relatively small number of samples have been analyzed, and that the study of a larger number of samples would have led to statistically more reliable results. However, only few studies have been carried out to date to compare the different preconcentration methods. We recommend that more studies are conducted in the future to test the different methods for quantifying the extraction efficiencies of Mn-cartridges.

Acknowledgements

The authors thank H el ene Planquette and Catherine Jeandel, PIs of the SWINGS project and chief scientist of the SWINGS cruise. We also thank the captain and the crew of the R/V Marion Dufresne for their assistance during the SWINGS cruise. The authors also thank Emmanuel de Saint-L eger and Fabien P erault, Marion Lagarde, Nolwenn Lemaitre, Edwin Cotard, Frederic Planchon for their help during the deployment of the *in-situ* pumps. We are grateful to Elodie Kestenare, Frederic Vivier, G erard Eldin, Sara Sergi, Corentin Clerc and Loyd Izard for CTD data acquisition and preparation of Niskin bottles. We thank Thomas Zambardi for his help at the LAFARA underground laboratory. The SWINGS project was supported by the French Oceanographic Fleet, ANR (Agence Nationale de la Recherche; ANR) CNRS/ INSU (Centre Nationale de la Recherche Scientifique/Institut National des Sciences de l'Univers) and ISblue (ANR-17-EURE-0015). This study has been partially supported through the grant EUR TESS N o ANR-18-EURE-0018 in the framework of the Programme des Investissements d'Avenir. M.A.C. was funded by the U.S. National Science Foundation OCE-2048067.

Authors contributions

The sampling design for fieldwork was conducted by PvB and VS. PvB, MS and ML mobilized equipment and consumables for fieldwork. Samples were collected in the field by PvB, VS and ML. Sample analysis was conducted by PvB, VS, ML, MS, MAC and PH. ML, PvB, VS and MAC analyzed and interpreted the data, ML produced the figures and wrote the paper. All authors provided comments on subsequent drafts of the paper.

Supplementary Material:

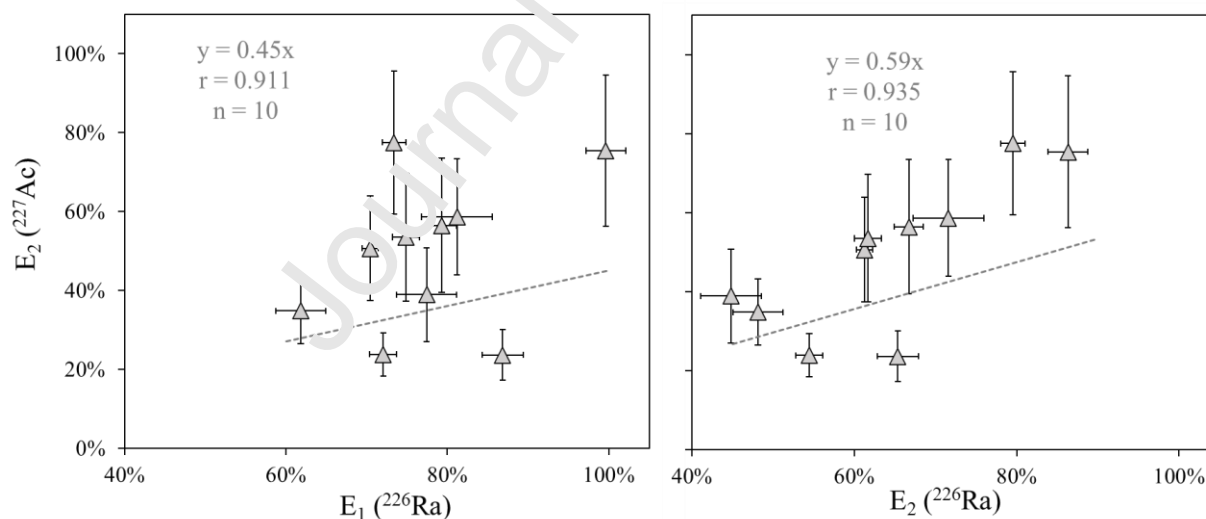


Figure S1: Comparison of the ^{227}Ac extraction efficiencies, $E_2(^{227}\text{Ac})$ as a function of $E_1(\text{Ra})$; on the left panel and as function of $E_2(\text{Ra})$ on the right panel. The grey dotted line shows the linear regression forced by the origin.

- Anderson, R.F., Bacon, M.P., Brewer, P.G., 1983. Removal of ^{230}Th and ^{231}Pa from the open ocean. *Earth Planet. Sci. Lett.* 62, 7–23. [https://doi.org/10.1016/0012-821X\(83\)90067-5](https://doi.org/10.1016/0012-821X(83)90067-5)
- Annett, A.L., Henley, S.F., Van Beek, P., Souhaut, M., Ganeshram, R., Venables, H.J., Meredith, M.P., Geibert, W., 2013. Use of radium isotopes to estimate mixing rates and trace sediment inputs to surface waters in northern Marguerite Bay, Antarctic Peninsula. *Antarct. Sci.* 25, 445–456. <https://doi.org/10.1017/S0954102012000892>
- Baskaran, M., Murphy, D.J., Santschi, P.H., Orr, J.C., Schink, D.R., 1993. A method for rapid in situ extraction and laboratory determination of Th, Pb, and Ra isotopes from large volumes of seawater. *Deep Sea Res. Part Oceanogr. Res. Pap.* 40, 849–865. [https://doi.org/10.1016/0967-0637\(93\)90075-E](https://doi.org/10.1016/0967-0637(93)90075-E)
- Bejannin, S., van Beek, P., Stieglitz, T., Souhaut, M., Tamborski, J., 2017. Combining airborne thermal infrared images and radium isotopes to study submarine groundwater discharge along the French Mediterranean coastline. *J. Hydrol. Reg. Stud.* 13, 72–90. <https://doi.org/10.1016/j.ejrh.2017.08.001>
- Bourquin, M., Van Beek, P., Reyss, J.-L., Souhaut, M., Charette, M.A., Jeandel, C., 2008. Comparison of techniques for pre-concentrating radium from seawater. *Mar. Chem.* 109, 226–237. <https://doi.org/10.1016/j.marchem.2008.01.002>
- Broecker, W.S., Goddard, J., Sarmiento, J.L., 1976. The distribution of ^{226}Ra in the Atlantic Ocean. *Earth Planet. Sci. Lett.* 32, 220–235. [https://doi.org/10.1016/0012-821X\(76\)90063-7](https://doi.org/10.1016/0012-821X(76)90063-7)
- Broecker, W.S., Li, Y.H., Cromwell, J., 1967. Radium-226 and Radon-222: Concentration in Atlantic and Pacific Oceans. *Science* 158, 1307–1310. <https://doi.org/10.1126/science.158.3805.1307>
- Charette, M.A., Dulaiova, H., Gonnee, M.E., Henderson, P.B., Moore, W.S., Scholten, J.C., Pham, M.K., 2012. GEOTRACES radium isotopes interlaboratory comparison experiment: Radium Intercomparison. *Limnol. Oceanogr. Methods* 10, 451–463. <https://doi.org/10.4319/lom.2012.10.451>
- Charette, M.A., Gonnee, M.E., Morris, P.J., Statham, P., Fones, G., Planquette, H., Salter, I., Garabato, A.N., 2007. Radium isotopes as tracers of iron sources fueling a Southern Ocean phytoplankton bloom. *Deep Sea Res. Part II Top. Stud. Oceanogr.* 54, 1989–1998. <https://doi.org/10.1016/j.dsr2.2007.06.003>
- Charette, M.A., Lam, P.J., Lohan, M.C., Kwon, E.Y., Hatje, V., Jeandel, C., Shiller, A.M., Cutter, G.A., Thomas, A., Boyd, P.W., Homoky, W.B., Milne, A., Thomas, H., Andersson, P.S., Porcelli, D., Tanaka, T., Geibert, W., Dehairs, F., Garcia-Orellana, J., 2016. Coastal ocean and shelf-sea biogeochemical cycling of trace elements and isotopes: lessons learned from GEOTRACES. *Philos. Trans. R. Soc. Math. Phys. Eng. Sci.* 374, 20160076. <https://doi.org/10.1098/rsta.2016.0076>
- Charette, M.A., Moran, S.B., 1999. Rates of particle scavenging and particulate organic carbon export estimated using ^{234}Th as a tracer in the subtropical and equatorial Atlantic Ocean. *Deep Sea Res. Part II Top. Stud. Oceanogr.* 46, 885–906. [https://doi.org/10.1016/S0967-0645\(99\)00006-5](https://doi.org/10.1016/S0967-0645(99)00006-5)
- Charette, M.A., Morris, P.J., Henderson, P.B., Moore, W.S., 2015. Radium isotope distributions during the US GEOTRACES North Atlantic cruises. *Mar. Chem.* 177, 184–195. <https://doi.org/10.1016/j.marchem.2015.01.001>
- Chung, Y., 1987. ^{226}Ra in the western Indian Ocean. *Earth Planet. Sci. Lett.* 85, 11–27. [https://doi.org/10.1016/0012-821X\(87\)90017-3](https://doi.org/10.1016/0012-821X(87)90017-3)

- Chung, Y., Craig, H., 1980. ^{226}Ra in the Pacific Ocean. *Earth Planet. Sci. Lett.* 49, 267–292. [https://doi.org/10.1016/0012-821X\(80\)90072-2](https://doi.org/10.1016/0012-821X(80)90072-2)
- Cochran, J.K., 1982. The oceanic chemistry of the U- and Th-series nuclides.
- Dulaiova, H., Ardelan, M.V., Henderson, P.B., Charette, M.A., 2009. Shelf-derived iron inputs drive biological productivity in the southern Drake Passage: SHELF-DERIVED IRON IN THE DRAKE PASSAGE. *Glob. Biogeochem. Cycles* 23, n/a-n/a. <https://doi.org/10.1029/2008GB003406>
- Dulaiova, H., Sims, K.W.W., Charette, M.A., Prytulak, J., Blusztajn, J.S., 2013. A new method for the determination of low-level actinium-227 in geological samples. *J. Radioanal. Nucl. Chem.* 296, 279–283. <https://doi.org/10.1007/s10967-012-2140-0>
- Elsinger, R.J., Moore, W.S., 1980. ^{226}Ra behavior in the Pee Dee River-Winyah Bay estuary. *Earth Planet. Sci. Lett.* 48, 239–249. [https://doi.org/10.1016/0012-821X\(80\)90187-9](https://doi.org/10.1016/0012-821X(80)90187-9)
- Garcia-Orellana, J., Rodellas, V., Tamborski, J., Diego-Feliu, M., van Beek, P., Weinstein, Y., Charette, M., Alorda-Kleinglass, A., Michael, H.A., Stieglitz, T., Scholten, J., 2021. Radium isotopes as submarine groundwater discharge (SGD) tracers: Review and recommendations. *Earth-Sci. Rev.* 220, 103681. <https://doi.org/10.1016/j.earscirev.2021.103681>
- Garcia-Solsona, E., Garcia-Orellana, J., Masqué, P., Dulaiova, H., 2008. Uncertainties associated with ^{223}Ra and ^{224}Ra measurements in water via a Delayed Coincidence Counter (RaDeCC). *Mar. Chem.* 22.
- Geibert, W., Charette, M., Kim, G., Moore, W.S., Miret, J., Young, M., Paytan, A., 2008. The release of dissolved actinium to the ocean: A global comparison of different end-members. *Mar. Chem.* 109, 409–420. <https://doi.org/10.1016/j.marchem.2007.07.005>
- Geibert, W., Rutgers van der Loeff, M.M., Hanfland, C., Dauelsberg, H.-J., 2002. Actinium-227 as a deep-sea tracer: sources, distribution and applications. *Earth Planet. Sci. Lett.* 198, 147–165. [https://doi.org/10.1016/S0012-821X\(02\)00512-5](https://doi.org/10.1016/S0012-821X(02)00512-5)
- Geibert, W., Vöge, I., 2008. Progress in the determination of ^{227}Ac in sea water. *Mar. Chem.* 109, 238–249. <https://doi.org/10.1016/j.marchem.2007.07.012>
- Gordon, Louis., Rowley, Keith., 1957. Coprecipitation of Radium with Barium Sulfate. *Anal. Chem.* 29, 34–37. <https://doi.org/10.1021/ac60121a012>
- Henderson, P.B., Morris, P.I., Moore, W.S., Charette, M.A., 2013. Methodological advances for measuring low-level radium isotopes in seawater. *J. Radioanal. Nucl. Chem.* 296, 357–362. <https://doi.org/10.1007/s10967-012-2047-9>
- Inoue, M., Hanaki, S., Kameyama, H., Kumamoto, Y., Nagao, S., 2022. Unique current connecting Southern and Indian Oceans identified from radium distributions. *Sci. Rep.* 12, 1781. <https://doi.org/10.1038/s41598-022-05928-y>
- Kadko, D., 1996. Radioisotopic studies of submarine hydrothermal vents. *Rev. Geophys.* 34, 349–366. <https://doi.org/10.1029/96RG01762>
- Kadko, D., Butterfield, D.A., 1998. The relationship of hydrothermal fluid composition and crustal residence time to maturity of vent fields on the Juan de Fuca Ridge. *Geochim. Cosmochim. Acta* 62, 1521–1533. [https://doi.org/10.1016/S0016-7037\(98\)00088-X](https://doi.org/10.1016/S0016-7037(98)00088-X)
- Kadko, D., Gronvold, K., Butterfield, D., 2007. Application of radium isotopes to determine crustal residence times of hydrothermal fluids from two sites on the Reykjanes Peninsula, Iceland. *Geochim. Cosmochim. Acta* 71, 6019–6029. <https://doi.org/10.1016/j.gca.2007.09.018>

- Kadko, D., Moore, W., 1988. Radiochemical constraints on the crustal residence time of submarine hydrothermal fluids: Endeavour Ridge. *Geochim. Cosmochim. Acta* 52, 659–668. [https://doi.org/10.1016/0016-7037\(88\)90328-6](https://doi.org/10.1016/0016-7037(88)90328-6)
- Kaufman, A., Trier, R.M., Broecker, W.S., Feely, H.W., 1973. Distribution of ^{228}Ra in the world ocean. *J. Geophys. Res.* 78, 8827–8848. <https://doi.org/10.1029/JC078i036p08827>
- Kemnitz, N.J., 2018. Actinium-227 as a tracer for mixing in the deep Northeast Pacific (Thesis of the requirements for the degree Master of science). University of Southern California.
- Key, R.M., Brewer, R.L., Stockwell, J.H., Guinasso, N.L., Schink, D.R., 1979a. Some improved techniques for measuring radon and radium in marine sediments and in seawater. *Mar. Chem.* 7, 251–264. [https://doi.org/10.1016/0304-4203\(79\)90042-2](https://doi.org/10.1016/0304-4203(79)90042-2)
- Key, R.M., Guinasso, N.L., Schink, D.R., 1979b. Emanation of radon-222 from marine sediments. *Mar. Chem.* 7, 221–250. [https://doi.org/10.1016/0304-4203\(79\)90041-0](https://doi.org/10.1016/0304-4203(79)90041-0)
- Kim, G., Ryu, J.-W., Yang, H.-S., Yun, S.-T., 2005. Submarine groundwater discharge (SGD) into the Yellow Sea revealed by ^{228}Ra and ^{226}Ra isotopes: Implications for global silicate fluxes. *Earth Planet. Sci. Lett.* 237, 156–166. <https://doi.org/10.1016/j.epsl.2005.06.011>
- Kipp, L.E., Charette, M.A., Hammond, D.E., Moore, W.S., 2015. Hydrothermal vents: A previously unrecognized source of actinium-227 to the deep ocean. *Mar. Chem.* 177, 583–590. <https://doi.org/10.1016/j.marchem.2015.09.002>
- Kipp, L.E., Charette, M.A., Moore, W.S., Henderson, P.B., Rigor, I.G., 2018a. Increased fluxes of shelf-derived materials to the central Arctic Ocean. *Sci. Adv.* 4, eaao1302. <https://doi.org/10.1126/sciadv.aao1302>
- Kipp, L.E., Sanial, V., Henderson, P.B., van Beek, P., Reyss, J.-L., Hammond, D.E., Moore, W.S., Charette, M.A., 2018b. Radium isotopes as tracers of hydrothermal inputs and neutrally buoyant plume dynamics in the deep ocean. *Mar. Chem.* 201, 51–65. <https://doi.org/10.1016/j.marchem.2017.06.011>
- Knauss, K.G., Ku, T.-L., Moore, W.S., 1978. Radium and thorium isotopes in the surface waters of the East Pacific and coastal Southern California. *Earth Planet. Sci. Lett.* 39, 235–249. [https://doi.org/10.1016/0012-821X\(78\)90199-1](https://doi.org/10.1016/0012-821X(78)90199-1)
- Koch-Larrouy, A., Atmadipoera, A., van Beek, P., Madec, G., Aucan, J., Lyard, F., Grelet, J., Souhaut, M., 2015. Estimates of tidal mixing in the Indonesian archipelago from multidisciplinary INDOMIX in-situ data. *Deep Sea Res. Part Oceanogr. Res. Pap.* 106, 136–153. <https://doi.org/10.1016/j.dsr.2015.09.007>
- Ku, T.L., Huh, C.A., Chou, P.S., 1980. Meridional distribution of ^{226}Ra in the eastern Pacific along GEOSECS cruise tracks. *Earth Planet. Sci. Lett.* 49, 293–308. [https://doi.org/10.1016/0012-821X\(80\)90073-4](https://doi.org/10.1016/0012-821X(80)90073-4)
- Ku, T.-L., Lin, M.-C., 1976. ^{226}Ra distribution in the Antarctic Ocean. *Earth Planet. Sci. Lett.* 32, 236–248. [https://doi.org/10.1016/0012-821X\(76\)90064-9](https://doi.org/10.1016/0012-821X(76)90064-9)
- Ku, T.-L., Mathieu, G.G., Knauss, K.G., 1977. Uranium in open ocean: concentration and isotopic composition. *Deep Sea Res.* 24, 1005–1017. [https://doi.org/10.1016/0146-6291\(77\)90571-9](https://doi.org/10.1016/0146-6291(77)90571-9)
- Le Roy, E., Sanial, V., Charette, M.A., van Beek, P., Lacan, F., Jacquet, S.H.M., Henderson, P.B., Souhaut, M., García-Ibáñez, M.I., Jeandel, C., Pérez, F.F., Sarthou, G., 2018. The ^{226}Ra –Ba relationship in the North Atlantic during GEOTRACES-GA01. *Biogeosciences* 15, 3027–3048. <https://doi.org/10.5194/bg-15-3027-2018>
- Le Roy, E., Sanial, V., Lacan, F., van Beek, P., Souhaut, M., Charette, M.A., Henderson, P.B., 2019. Insight into the measurement of dissolved ^{227}Ac in seawater using radium delayed

- coincidence counter. *Mar. Chem.* 212, 64–73.
<https://doi.org/10.1016/j.marchem.2019.04.002>
- Le Roy, E., van Beek, P., Lacan, F., Souhaut, M., Sanial, V., Charette, M.A., Henderson, P.B., Deng, F., 2023. The distribution of ^{227}Ac along the GA01 section in the North Atlantic. *Mar. Chem.* 248, 104207. <https://doi.org/10.1016/j.marchem.2023.104207>
- Léon, M., Beek, P., Scholten, J., Moore, W.S., Souhaut, M., De Oliveira, J., Jeandel, C., Seyler, P., Jouanno, J., 2022. Use of ^{223}Ra and ^{224}Ra as chronometers to estimate the residence time of Amazon waters on the Brazilian continental shelf. *Limnol. Oceanogr.* 67, 753–767. <https://doi.org/10.1002/lno.12010>
- Levier, M., Roy-Barman, M., Colin, C., Dapoigny, A., 2021. Determination of low level of actinium 227 in seawater and freshwater by isotope dilution and mass spectrometry. *Mar. Chem.* 233, 103986. <https://doi.org/10.1016/j.marchem.2021.103986>
- Li, Y.-H., Chan, L.-H., 1979. Desorption of Ba and ^{226}Ra from river borne sediments in the Hudson estuary. *Earth Planet. Sci. Lett.* 43, 343–350. [https://doi.org/10.1016/0012-821X\(79\)90089-X](https://doi.org/10.1016/0012-821X(79)90089-X)
- Li, Y.-H., Feely, H.W., Toggweiler, J.R., 1980. ^{228}Ra and ^{228}Th concentrations in GEOSECS Atlantic surface waters. *Deep Sea Res. Part Oceanogr. Res. Pap.* 27, 545–555.
[https://doi.org/10.1016/0198-0149\(80\)90039-4](https://doi.org/10.1016/0198-0149(80)90039-4)
- Livingston, H.D., Cochran, J.K., 1987. Determination of uranium and thorium isotopes in ocean water: In solution and in filterable particles. *J. Radioanal. Nucl. Chem. Artic.* 115, 299–308. <https://doi.org/10.1007/BF02037115>
- Mann, D.R., Casso, S.A., 1984. In situ chemisorption of radiocesium from seawater. *Mar. Chem.* 14, 307–318. [https://doi.org/10.1016/0304-4203\(84\)90027-6](https://doi.org/10.1016/0304-4203(84)90027-6)
- Moore, W.S., 2008. Fifteen years experience in measuring ^{224}Ra and ^{223}Ra by delayed-coincidence counting. *Mar. Chem.* 109, 188–197.
<https://doi.org/10.1016/j.marchem.2007.06.015>
- Moore, W.S., 1987. Radium 228 in the South Atlantic Bight. *J. Geophys. Res.* 92, 5177.
<https://doi.org/10.1029/JC092i05p05177>
- Moore, W.S., 1976. Sampling ^{228}Ra in the deep ocean. *Deep Sea Res. Oceanogr. Abstr.* 23, 647–651. [https://doi.org/10.1016/0011-7471\(76\)90007-3](https://doi.org/10.1016/0011-7471(76)90007-3)
- Moore, W.S., 1969. Oceanic concentrations of ^{228}Ra . *Earth Planet. Sci. Lett.* 6, 437–446.
[https://doi.org/10.1016/0012-821X\(69\)90113-7](https://doi.org/10.1016/0012-821X(69)90113-7)
- Moore, W.S., Cai, P., 2013. Calibration of RaDeCC systems for ^{223}Ra measurements. *Mar. Chem.* 156, 130–137. <https://doi.org/10.1016/j.marchem.2013.03.002>
- Moore, W.S., Krest, J., 2004. Distribution of ^{223}Ra and ^{224}Ra in the plumes of the Mississippi and Atchafalaya Rivers and the Gulf of Mexico. *Mar. Chem.* 86, 105–119.
<https://doi.org/10.1016/j.marchem.2003.10.001>
- Moore, W.S., Reid, D.F., 1973. Extraction of radium from natural waters using manganese-impregnated acrylic fibers. *J. Geophys. Res.* 78, 8880–8886.
<https://doi.org/10.1029/JC078i036p08880>
- Moore, W.S., Sarmiento, J.L., Key, R.M., 2008a. Submarine groundwater discharge revealed by ^{228}Ra distribution in the upper Atlantic Ocean. *Nat. Geosci.* 1, 309–311.
<https://doi.org/10.1038/ngeo183>
- Moore, W.S., Ussler, W., Paull, C.K., 2008b. Short-lived radium isotopes in the Hawaiian margin: Evidence for large fluid fluxes through the Puna Ridge. *Mar. Chem.* 109, 421–430. <https://doi.org/10.1016/j.marchem.2007.09.010>

- Neff, J.M., 2002. Radium Isotopes in the Ocean, in: *Bioaccumulation in Marine Organisms*. Elsevier, pp. 191–201. <https://doi.org/10.1016/B978-008043716-3/50012-9>
- Nozaki, Y., 1993. Actinium-227: A Steady State Tracer for the Deep-sea Basin-wide Circulation and Mixing Studies, in: *Elsevier Oceanography Series*. Elsevier, pp. 139–156. [https://doi.org/10.1016/S0422-9894\(08\)71323-0](https://doi.org/10.1016/S0422-9894(08)71323-0)
- Nozaki, Y., 1984. Excess ^{227}Ac in deep ocean water. *Nature* 310, 486–488. <https://doi.org/10.1038/310486a0>
- Peterson, R.N., Burnett, W.C., Dimova, N., Santos, I.R., 2009. Comparison of measurement methods for radium-226 on manganese-fiber: Methods for ^{226}Ra analysis on Mn-fiber. *Limnol. Oceanogr. Methods* 7, 196–205. <https://doi.org/10.4319/lom.2009.7.196>
- Reid, D.F., Key, R.M., Schink, D.R., 1979. Radium, thorium, and actinium extraction from seawater using an improved manganese-oxide-coated fiber. *Earth Planet. Sci. Lett.* 43, 223–226. [https://doi.org/10.1016/0012-821X\(79\)90205-X](https://doi.org/10.1016/0012-821X(79)90205-X)
- Rodellas, V., Garcia-Orellana, J., Trezzi, G., Masqué, P., Stieglitz, T.C., Bokuniewicz, H., Cochran, J.K., Berdalet, E., 2017. Using the radium quotient to quantify submarine groundwater discharge and porewater exchange. *Geochim. Cosmochim. Acta* 196, 58–73. <https://doi.org/10.1016/j.gca.2016.09.016>
- Sanial, V., Kipp, L.E., Henderson, P.B., van Beek, P., Reys, J.-L., Hammond, D.E., Hawco, N.J., Saito, M.A., Resing, J.A., Sedwick, P., Moore, W.S., Charette, M.A., 2018. Radium-228 as a tracer of dissolved trace element inputs from the Peruvian continental margin. *Mar. Chem.* 201, 20–34. <https://doi.org/10.1016/j.marchem.2017.05.008>
- Sanial, V., van Beek, P., Lansard, B., d'Ovidio, F., Kestenare, E., Souhaut, M., Zhou, M., Blain, S., 2014. Study of the phytoplankton plume dynamics off the Crozet Islands (Southern Ocean): A geochemical-physical coupled approach. *J. Geophys. Res. Oceans* 119, 2227–2237. <https://doi.org/10.1002/2013JC009305>
- Sanial, V., van Beek, P., Lansard, B., Souhaut, M., Kestenare, E., d'Ovidio, F., Zhou, M., Blain, S., 2015. Use of Ra isotopes to reduce rapid transfer of sediment-derived inputs off Kerguelen. *Biogeosciences* 12, 1415–1430. <https://doi.org/10.5194/bg-12-1415-2015>
- Shaw, T.J., Moore, W.S., 2002. Analysis of ^{227}Ac in seawater by delayed coincidence counting. *Mar. Chem.* 78, 197–203. [https://doi.org/10.1016/S0304-4203\(02\)00022-1](https://doi.org/10.1016/S0304-4203(02)00022-1)
- Tamborski, J.J., Cochran, J.K., Bokuniewicz, H.J., 2017. Application of ^{224}Ra and ^{222}Rn for evaluating seawater residence times in a tidal subterranean estuary. *Mar. Chem.* 189, 32–45. <https://doi.org/10.1016/j.marchem.2016.12.006>
- van Beek, P., Bourquin, M., Reys, J.-L., Souhaut, M., Charette, M.A., Jeandel, C., 2008. Radium isotopes to investigate the water mass pathways on the Kerguelen Plateau (Southern Ocean). *Deep Sea Res. Part II Top. Stud. Oceanogr.* 55, 622–637. <https://doi.org/10.1016/j.dsr2.2007.12.025>
- van Beek, P., Souhaut, M., Lansard, B., Bourquin, M., Reys, J.-L., von Ballmoos, P., Jean, P., 2013. LAFARA: a new underground laboratory in the French Pyrénées for ultra low-level gamma-ray spectrometry. *J. Environ. Radioact.* 116, 152–158. <https://doi.org/10.1016/j.jenvrad.2012.10.002>
- van der Loeff, M.M.R., Moore, W.S., 1999. Determination of natural radioactive tracers, in: Grasshoff, K., Kremling, K., Ehrhardt, M. (Eds.), *Methods of Seawater Analysis*. Wiley-VCH Verlag GmbH, Weinheim, Germany, pp. 365–397. <https://doi.org/10.1002/9783527613984.ch13>

- Vieira, L.H., Krisch, S., Hopwood, M.J., Beck, A.J., Scholten, J., Liebetrau, V., Achterberg, E.P., 2020. Unprecedented Fe delivery from the Congo River margin to the South Atlantic Gyre. *Nat. Commun.* 11, 556. <https://doi.org/10.1038/s41467-019-14255-2>
- Weyer, S., Anbar, A.D., Gerdes, A., Gordon, G.W., Algeo, T.J., Boyle, E.A., 2008. Natural fractionation of $^{238}\text{U}/^{235}\text{U}$. *Geochim. Cosmochim. Acta* 72, 345–359. <https://doi.org/10.1016/j.gca.2007.11.012>
- Yamada, M., Nozaki, Y., 1986. Radium isotopes in coastal and open ocean surface waters of the Western North Pacific. *Mar. Chem.* 19, 379–389. [https://doi.org/10.1016/0304-4203\(86\)90057-5](https://doi.org/10.1016/0304-4203(86)90057-5)

Journal Pre-proof

Journal Pre-proof

Table 1: ^{226}Ra activities (in dpm 100L^{-1}) determined in Mn-fibers and in A and B Mn-cartridges; the extraction efficiencies E_1 (Ra) (derived from Equation 1) and E_2 (Ra) (derived from Equation 5) determined for each depth are also reported. No data were available (n.a.) at 500 m at station 15 (Mn-

Station	Depth (m)	^{226}Ra		Volume (L)	^{226}Ra		Volume (L)	^{226}Ra		Extraction efficiency			
		Mn-fibers (dpm 100L^{-1})			A Mn-cartridge (dpm 100L^{-1})			B Mn-cartridge (dpm 100L^{-1})		E_1 (%)	E_2 (%)		
14	50	11	0.	427	10.	0.1	n.a.	94	2.	.5	± 8	n.a.	
		.1 ± 3			5 ± 3								
	210	13	0.	601	11.	0.1	n.a.	84	1.	.8	± 7	n.a.	
		.2 ± 2			2 ± 2								
	900	15	0.	615	11.	0.0	n.a.	73	3.	.5	± 1	n.a.	
		.3 ± 6			2 ± 7								
	100	17	0.	528	10.	0.1	5	0.0	61	3.	48	0.	
		.3 ± 8			7 ± 2	5 ± 8	.8 ± 1	.1 ± 9					
	110	15	0.	548	13.	0.1	4.	0.0	86	2.	65	1.	
		.5 ± 4			4 ± 4	7 ± 8	.8 ± 5	.4 ± 2					
	116	14	0.	584	11.	0.1	6.	0.0	77	3.	44	0.	
		.2 ± 7			5 ± 2	1 ± 8	.4 ± 7	.8 ± 8					
120	16	0.	674	11.	0.1	4.	0.0	70	1.	61	1.		
	.8 ± 2			8 ± 2	6 ± 7	.5 ± 0	.3 ± 1						
126	15	0.	645	11.	0.1	5.	0.0	72	1.	54	1.		
	.5 ± 3			2 ± 1	1 ± 8	.1 ± 7	.5 ± 0						
15	700		532	10.	0.1	3.	0.0	n.a.				62	1.
					6 ± 2	9 ± 7						.9 ± 3	
	116	15	0.	579	15.	0.1	2.	0.0	99	2.	86	2.	
		.8 ± 4			8 ± 5	2 ± 5	.6 ± 5	.3 ± 2					
	120	16	0.	503	13.	0.1	4.	0.0	79	1.	66	1.	
		.5 ± 3			1 ± 4	4 ± 8	.3 ± 8	.7 ± 3					
	126	17	0.	665	14.	0.1	4.	0.0	81	4.	71	1.	
		.5 ± 9			2 ± 4	0 ± 6	.2 ± 4	.6 ± 3					
	137	16	0.	677	12.	0.1	4.	0.0	74	1.	61	1.	
		.2 ± 3			1 ± 2	6 ± 7	.9 ± 7	.7 ± 1					
169	17	0.	630	12.	0.1	2.	0.0	73	1.	79	1.		
	.4 ± 3			8 ± 3	6 ± 5	.4 ± 5	.5 ± 6						
								Me	79	10	63	12	
								an	.2 ± .3	.9 ± .4			

fibers) and at 50, 210, 900 m depth at station 14 (Mn-cartridges).

Journal Pre-proof

Table. 2: ^{227}Ac activities determined in the A and B Mn-cartridges (Act_A and Act_B , respectively, in $\text{dpm } 100\text{L}^{-1}$) together with the extraction efficiency - $E_2(^{227}\text{Ac})$ - deduced from Equation 5.

Station	Depth (m)	Volume (L)	^{227}Ac		Extraction Efficiency $E_2(^{227}\text{Ac})$ (%)
			A Mn-cartridge ($\text{dpm } 100\text{L}^{-1}$)	B Mn-cartridge ($\text{dpm } 100\text{L}^{-1}$)	
14	1000	528	0.013 ± 0.002	0.008 ± 0.002	34.8 ± 8.3
	1100	548	0.015 ± 0.003	0.012 ± 0.002	23.7 ± 6.4
	1160	584	0.009 ± 0.002	0.006 ± 0.001	38.9 ± 11.9
	1200	674	0.018 ± 0.003	0.009 ± 0.002	50.7 ± 13.3
	1260	646	0.021 ± 0.004	0.016 ± 0.002	23.8 ± 5.5
15	1160	579	0.022 ± 0.003	0.005 ± 0.001	75.4 ± 19.2
	1200	503	0.016 ± 0.003	0.007 ± 0.002	56.4 ± 17.0
	1260	665	0.022 ± 0.004	0.009 ± 0.002	58.6 ± 14.7
	1370	677	0.013 ± 0.003	0.006 ± 0.001	53.5 ± 16.2
	1690	630	0.043 ± 0.007	0.010 ± 0.002	77.5 ± 18.1
Mean					49.3 ± 19.0

- We compare methods to estimate Ra and ^{227}Ac extraction efficiency of Mn-cartridges.
- The Ra extraction efficiencies of the Mn-cartridges range from 44.8 % to 99.6 %.
- The ^{227}Ac extraction efficiencies are lower than those for Ra (23.7-77.5 %).
- The ^{227}Ac extraction efficiency can be estimated from the Ra extraction efficiency.

Journal Pre-proof